PKCε Phosphorylation of RyR2:

A Novel Link between Diabetes and Arrhythmia.

Alexander Wong

Supervisor: Dr. Peter Jones

A thesis submitted in partial fulfilment for the degree of

Bachelor of Biomedical Science with Honours University of Otago

Dunedin, New Zealand

October 2017

Abstract

Cardiovascular disease (CVD) is the leading cause of death in the world. Arrhythmia is a type of CVD which can be caused by store overload induced calcium (Ca^{2+}) release (SOICR) in cardiomyocytes. SOICR occurs through the cardiac ryanodine receptor (RyR2). RyR2 phosphorylation is known to be a cause of SOICR. Patients with diabetes (DM) have an increased risk of arrhythmia as well as an increase in RyR2 phosphorylation by certain kinases. One kinase activated in DM is Protein Kinase C (PKC). PKC isoforms; α, ε, β_2 and δ have an increased activity in the DM heart. Our study aimed to determine the effect of PKC on RyR2 in regard to SOICR. We hypothesised that activation or overexpression of PKC would result in an increase in SOICR consistent with RyR2 phosphorylation by other kinases. SOICR was examined in HEK293 cells expressing RyR2 with or without PKC overexpression in the presence and absence of a PKC activator (Dic8) and inhibitor (Go6983). Dic8, as well as Go6983, resulted in an increase in the occurrence of SOICR. Recent studies in the lab show that ATP analogues directly affect RyR2 resulting in SOICR, making the results of Go6983 hard to interpret. Overexpression of PKCα, with or without Dic8, resulted in small increase in the occurrence of SOICR. However, overexpression of PKCε, with or without Dic8, resulted in a large increase in the occurrence of SOICR. The propensity for SOICR is determined by the sensitivity of RyR2 to sarcoplasmic reticulum (SR) Ca^{2+}. To study if PKC altered the sensitivity of RyR2 to SR Ca^{2+} a SR targeted Ca^{2+} sensing protein, D1ER, was used. Overexpression of PKCα resulted in no change in the sensitivity of RyR2 to SR Ca^{2+}, however, consistent with the increase in the propensity for SOICR, PKCε resulted in an increase in the sensitivity of RyR2 to SR Ca^{2+}. Our data indicate that akin to other kinases, PKCε can increase SOICR through the RyR2 due to an increase in RyR2's sensitivity to SR Ca^{2+}. These findings may represent a novel link through which DM mediated changes in cell signalling increase the risk of arrhythmias.

Acknowledgements

Firstly, I would like to give my thanks and appreciation to my supervisor Dr. Peter Jones. Thank you for always having your door open to me when I needed help. I am very grateful for all the ongoing support, constructive feedback and guidance you have given me throughout this year. I am grateful to have been a part of such stimulating research in the Jones Laboratory.

Many thanks to Janet McLay, our assistant research fellow, for giving up her time to teach me the experimental protocols that I needed for my project. I would also like to thank the rest of the Jones Laboratory; Akash Chakraborty, Luis Gonano, Michelle Munro and Callum Tanner, for not only their expertise and the enormous help they have given me throughout this year, but also the close friendships I have formed with them.

To the Department of Physiology and the School of Biomedical Sciences, thank you for the opportunities I have been given and the environment you have provided to allow me to grow and thrive. Through the School of Biomedical Sciences, I am honoured to have received the inaugural Elizabeth Jean Trotter Scholarship, donated by Dr. Hugh Bodle, that has helped me immensely with my finances as well as my confidence in my ability to succeed.

To my wonderful and beautiful Fiancé, Mika Smith, and my family; thank you for your support, strength, and belief in me. To my fellow honours students; Kevin Jagau, Hamish Aitken-Buck, Caitlin Arpel and Rachael Iremonger, thank you for your companionship. I have enjoyed all our cheerful conversations through a tough yet exciting year.

I would like to dedicate this thesis to my beloved uncle, Francis Wong, whom sadly passed away in late November this year.

Table of Contents

List of Figures

List of Tables

List of Abbreviations

AF	Atrial Fibrillation
AFL	Atrial Flutter
AGE	Advanced Glycated End Products
ANOVA	Analysis of Variance
aPKC	Atypical PKC
APS	Ammonium Persulfate
AV	Atrioventricular
BSA	Bovine Serum Albumin
Ca^{2+}	Calcium Ion
CaMKII	Ca^{2+}/Calmodulin-Dependant Protein Kinase II
CFP	Cyan Fluorescent Protein
CICR	Ca^{2+} Induced Ca^{2+} Release
CPC	Cardiac Pacemaker Cells
cPKC	Conventional PKC
CPVT	Catecholaminergic Polymorphic Ventricular Tachycardia
CVD	Cardiovascular Disease
DAD	Delayed After Depolarisation
Dic8	1,2-Dioctanoyl-sn-Glycerol
DM	Diabetes Mellitus
DMEM	Dulbecco's Modified Eagle's Medium
EDTA	Ethylenediaminetetraacetic Acid
F	Fluorescence Resonance Energy Transfer
FBS	Fetal Bovine Serum
GAPDH	Glyceraldehyde 3-Phosphate Dehydrogenase
GPCR-αq	G-Protein Coupled Receptor αq

HEK293	Human Embryonic Kidney 293
HRP	Horseradish Peroxidase
IP3	Inositol 1,4,5-Triphosphate
KRH	Krebs-Ringer HEPES
NCX	Na^{+} Ca^{2+} Exchanger
NEAA	Non-Essential Amino Acids
n	Sample Size
nPKC	Novel PKC
PAGE	Polyacrylamide Gel Electrophoresis
PBS	Phosphate Buffered Saline
PBS-T	PBS Tween-20
PDK1	Pyruvate Dehydrogenase Kinase 1
PIP2	Inositol Phospholipids
PIP3	Phosphatidylinositol (3,4,5)-Trisphosphate
PKA	Protein Kinase A
PKC	Protein Kinase C
PKG	Protein Kinase G
PLC	Phospholipase-C
PM	Plasma Membrane
PMCA	Plasma Membrane Ca^{2+} ATPase
RA	Right Atrium
ROI	Region of Interest
RyR2	Ryanodine Receptor 2
S	Serine Residue
SA	Sinoatrial
SB	Sample Buffer

SEM	Standard Error of the Mean
SERCA	Sarco/Endoplasmic Reticulum Ca^{2+} ATPase
SDS	Sodium Dodecyl Sulfate
SOICR	Store Overload-Induced Ca^{2+} Release
SR	Sarcoplasmic Reticulum
TEMED	Tetramethylethylenediamine
YFP	Yellow Fluorescent Protein

1 Introduction

1.1 Diabetes

Diabetes mellitus (DM) is a disease characterised by hyperglycemia, and is clinically diagnosed as a fasting blood plasma glucose level ≥7.0 mmol/L (Zimmet *et al.*, 2001). There are two types of DM; type 1, a T-lymphocyte autoimmune disease which accounts for approximately 10% of all DM, and type 2 a metabolic disorder which accounts for approximately 90% of all DM (Zimmet *et al.*, 2001). The worldwide prevalence of DM has almost doubled from 1980 (4.7%) to 2014 (8.5%) and is still on the rise (NCD Risk Factor Collaboration, 2016). In 2014, it was estimated 3.7 million deaths were attributed to DM worldwide where over 50% were cardiovascular disease (CVD) related (NCD Risk Factor Collaboration, 2016).

1.1.1 Diabetic Heart Disease

Patients with DM are known to have many CVD's, including; microangiopathy, macroangiopathy, cardiomyopathy, and arrhythmias, all of which are related due to many molecular and biochemical changes that can occur in hyperglycemic environments (Grundy *et al.*, 1999). Diabetic micro/macro-angiopathy has been well described in the literature, as most DM patients will experience some form of vessel dysfunction, which can result in retinopathy, nephropathy, or neuropathy (Alonso-Moran *et al.*, 2014). In addition to vessel disease, one epidemiological study comparing 293,124 DM against 552,624 non-DM hospitalized patients, between the years 1990 and 2000, showed an increase in the percent occurrences of atrial fibrillation (AF) and atrial flutter (AFL) in DM compared to the non-DM (14.9% versus 10.3%, and 4% versus 2.5%, respectively) (Movahed *et al.*, 2005). The increased association and risk of arrhythmia in DM patients increases the risk of heart failure and death in these patients (Siscovick *et al.*, 2010).

1.2 Contraction of the Heart

1.2.1 Heart Conduction

The heart beats due to spontaneous electrical activity generated by cardiac pacemaker cells (CPCs) in the sinoatrial (SA) node, located in the upper region of the right atrium (RA). CPCs in the SA node generate a wave of electrical activity which propagates down towards the atrioventricular (AV) node, located in the lower region of the RA (Figure 1.1). Here, the wave of electrical activity is then sent down the bundle of His fibres which are located within the intraventricular septum, before moving through the Purkinje fibres which are located around the walls of the left and right ventricular walls (Figure 1.1). Electrical stimulation of cardiomyocytes results in a coordinated contraction of the myocardium, as cardiomyocytes are all connected by intercalated discs that contain desmosomes (physical connection) and gap junctions (electrical connection) (Saffitz, 2005). This process results in rhythmic contraction and relaxation of the heart.

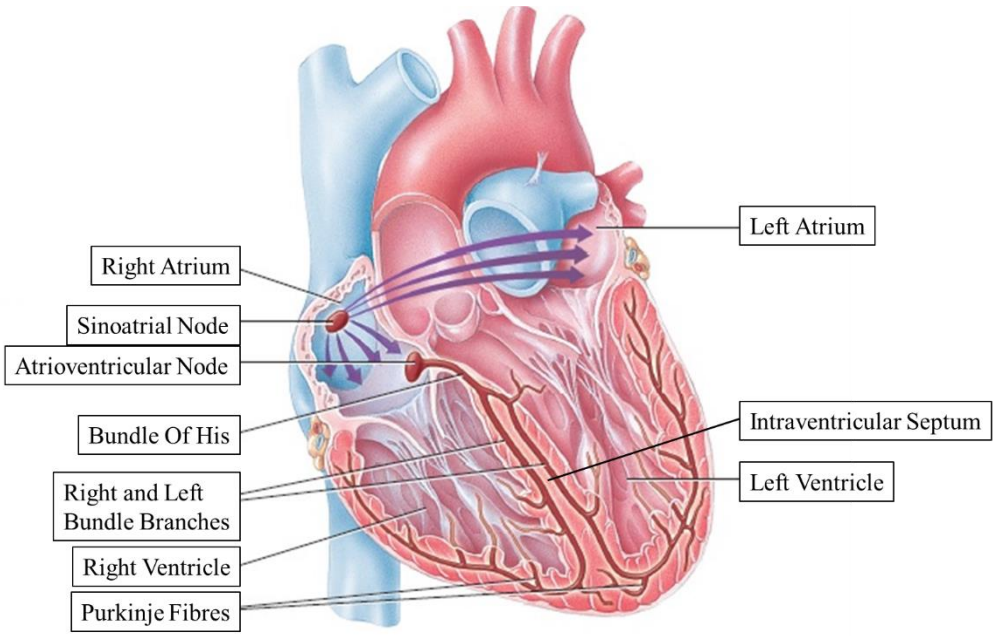

Figure 1.1 Conduction of the Heart.

CPCs in the SA node send electrical activity that propagates down to the AV node followed by the Bundle of His then through the Purkinje fibres in the left and right ventricles. Adapted from Wiley *et al*., 2011.

1.2.2 Excitation-Contraction Coupling

The propagating electrical signal must be converted to a chemical one to drive contraction; this process is known as excitation-contraction coupling (Sandow, 1952). Electrical activity generated by the pacemaker cells in the heart described in Section 1.2.1, results in a change in the membrane potential at the level of cardiomyocytes resulting in the opening of voltage-gated L-type calcium (Ca^{2+}) channels on the plasma membrane (PM), slightly raising the tightly regulated Ca^{2+} concentration in the cytosol (Figure 1.2) (Aronsen *et al.*, 2013). This slight Ca^{2+} increase activates the ryanodine receptor 2 (RyR2), which is a Ca^{2+} release channel located on the sarcoplasmic reticulum (SR) membrane (Figure 1.2) (Zhang *et al.*, 2015). Activation of the RyR2 causes a large amount of Ca^{2+} to be released into the cytosol from the SR, a process termed Ca^{2+} induced Ca^{2+} release (CICR), which is sufficient for contraction of the heart (Figure 1.2) (Aronsen *et al.*, 2013). The high Ca^{2+} concentration in the cytosol is then either recycled into the SR by the sarco/endoplasmic reticulum Ca^{2+} ATPase (SERCA) or extruded out of the cell through the Na^{+} Ca^{2+} exchanger (NCX) or the PM Ca^{2+} ATPase (PMCA) channel, to prepare for the sequential contraction of the heart (Figure 1.2) (Eisner *et al.*, 2013).

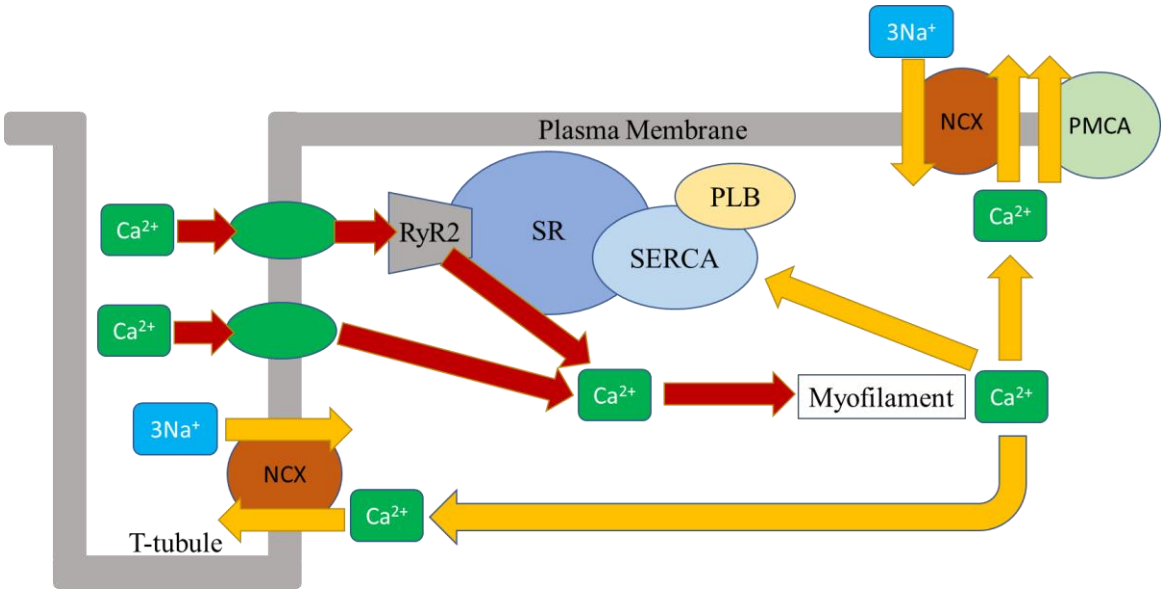

Figure 1.2 Excitation Contraction Coupling.
The opening of the LTCC after depolarisation of the PM allows for Ca^{2+} entry into the cardiomyocyte. Ca^{2+} activates the RyR2 allowing for CICR from the SR. Ca^{2+} binds to the myofilament allowing for contraction of the cell. Ca^{2+} is then recycled into the SR via SERCA and removed from the cell via the NCX and PMCA. Created with Microsoft PowerPoint.

1.3 Arrhythmia

Cardiac arrhythmia is a CVD characterised by an irregular heartbeat, which can be clinically diagnosed using electrocardiography, where any changes in the normal conduction of the heart, described in Section 1.2.1, is considered cardiac arrhythmia (Grace & Roden, 2012). There are many factors that can cause arrhythmia, however, one underlying factor is the disruption of Ca^{2+} handling proteins in cardiomyocytes (Wagner *et al.*, 2015). In particular, an increased activity of the RyR2 can result in arrhythmia due to spontaneous Ca^{2+} leak from the SR (Jones *et al.*, 2008). The clinical implications of arrhythmia can vary from mild outcomes, such as reducing the quality of life, to severe outcomes including sudden cardiac death (Grace & Roden, 2012).

1.3.1 Store Overload Induced Ca^{2+} Release

Modification of Ca^{2+} handling proteins involved in CICR; including RyR2, PLB, and SERCA mentioned in Section 1.2.2, have been attributed to the un-stimulated leak of Ca^{2+} from the SR (Aschar-Sobbi *et al.*, 2012; Shan *et al.*, 2012). The un-stimulated Ca^{2+} release is referred to as spontaneous Ca^{2+} release, or due to its dependence on SR Ca^{2+} levels, store overload-induced Ca^{2+} release (SOICR) (Belke *et al.*, 2004; Jones *et al.*, 2008). Normally the SR is never filled to maximum, rather it has a certain level of Ca^{2+} within the store (Figure 1.3 A) (Jones *et al.*, 2008). If the Ca^{2+} level within the SR increases and surpasses a certain release threshold or SOICR threshold, it results in the activation of the RyR2 resulting in SOICR. The amount of Ca^{2+} released from the SR is determined by the termination of SOICR (termination threshold) (Palade *et al.*, 1983). Modifications of RyR2 can result in the reduction of this Ca^{2+} release threshold in the SR, below the SR Ca^{2+} load which then can cause SOICR seen in Figure 1.3 B. Modifications of PLB and SERCA can result in SOICR due to overloading Ca^{2+} levels within the SR, surpassing the Ca^{2+} release threshold (Jones *et al.*, 2008). RyR2 modifications can also

result in a reduction in the termination threshold, resulting in an increased amount of Ca^{2+} every time RyR2 is activated seen in Figure 1.3 C (Tang *et al.*, 2012). A reduction of termination threshold does not result in SOICR, however, the combination of reduced termination threshold along with release threshold would result in an increased occurrence of SOICR along with a high amount of Ca^{2+} leak resulting in elevated cytosolic Ca^{2+} levels, Figure 1.3 D.

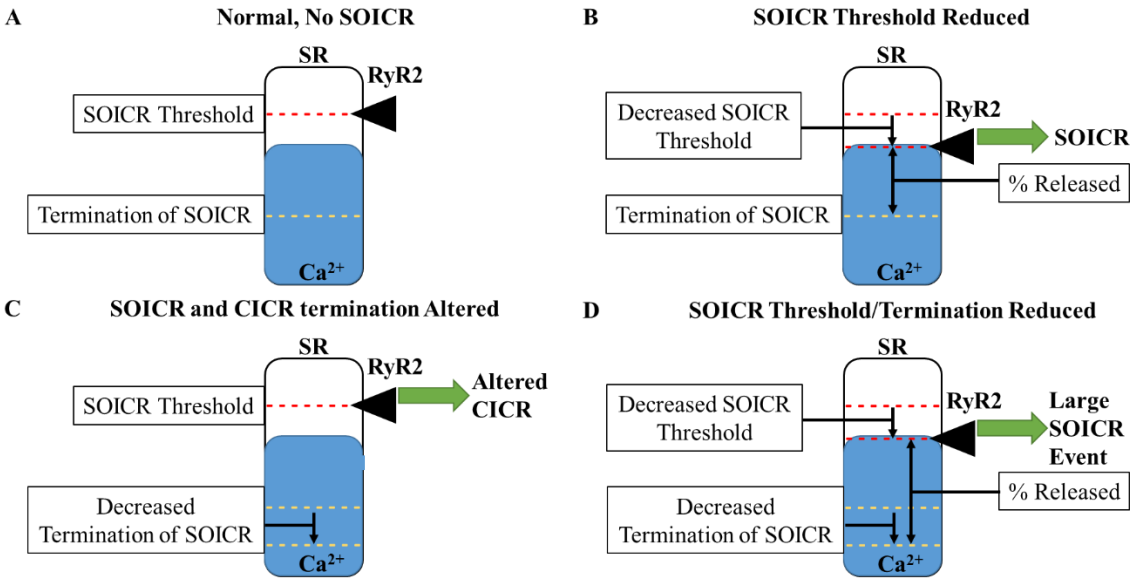

Figure 1.3 SOICR.
(A) The SR is filled with a certain level of Ca^{2+} (blue) where if this level would increase over the SOICR threshold it would result in SOICR. After activation of the RyR2 in CICR, only a proportion of Ca^{2+} is released to ensure the SR does not get emptied completely. (B) Modification of the RyR2 can result in a reduction of the SOICR threshold, increasing the occurrence of SOICR. (C) Modification of RyR2 can result in a reduction in termination of SOICR, releasing a higher proportion of Ca^{2+} when activated. (D) A combination of a decreased SOICR threshold and termination of SOICR results high a large SOICR event. Created with Microsoft PowerPoint.

As Ca^{2+} levels are tightly regulated in the cytosol of cardiomyocytes, an increase in Ca^{2+} release due to SOICR must be adequately removed by an increase of SERCA or the NCX activity. An increase in SERCA activity is not effective at reducing the Ca^{2+} levels, as an increased uptake of Ca^{2+} into the SR would result in a sequential SOICR event. As a result, the high amounts of Ca^{2+} in the cytosol must be extruded by increased activity of NCX (Venetucci *et al.*, 2007). NCX is effective at maintaining the Ca^{2+} levels during SOICR events, however, because it is

an electrogenic exchanger, one Ca^{2+} ion out of the cytosol into the extracellular space for three Na^{+} ions from the extracellular space into the cytosol, removal of high amounts of Ca^{2+} results in an elevated level of Na^{+} within the cytosol (Venetucci *et al.*, 2007). An increase of cations within the cytosol causes an increase in the membrane potential, which can then result in the depolarization of the cardiomyocyte membrane, considered as delayed after depolarisation (DAD) (Bers, 2002; Belke *et al.*, 2004; Venetucci *et al.*, 2007). If there are enough cardiomyocytes experiencing DAD's, the electrical depolarization can be propagated throughout the whole heart due to the electrical connection between the cardiomyocytes (Saffitz, 2005). The occurrence of these DAD's throughout the whole heart leads to contraction of the heart, in the absence of a pacemaker depolarization wave, resulting in arrhythmia (Houser, 2000).

1.3.2 RyR2 Modifications

RyR is a homo-tetrameric protein and is the largest known ion channel (2.2MDa) and exists as three isoforms, RyR1, RyR2 and RyR3, where RyR2 is mainly expressed in cardiomyocytes (Bers, 2004; Van Petegem, 2015). The RyR2 monomer is made up of approximately 5,000 amino-acids, therefore it is proposed and expected that there are many potential sites for post-translational modifications including; phosphorylation, oxidation, and glycation (Jones *et al.*, 2008; Van Petegem, 2015). Under normal physiological conditions, the RyR2 is phosphorylated at a basal level, however, in pathophysiological conditions where kinases such as Ca^{2+}/calmodulin-dependant protein kinase II (CaMKII) and protein kinase A (PKA) are overexpressed or excessively active, the RyR2 is hyperphosphorylated (Wehrens *et al.*, 2006). Although there are predicted to be many phosphorylation residues within RyR2, only three phosphorylation residues have been reported to date; serine (S) 2808, S2814 and S2030, all of which have been studied extensively for CaMKII and PKA (Figure 1.4) (Huke & Bers, 2008; Valdivia, 2012). CaMKII and PKA are kinases that phosphorylate serine/threonine residues and

are normally auto-inhibited due to their respective regulatory domain blocking the catalytic sites of the kinase (Zhang *et al.*, 2012; Erickson, 2014). There is a large debate on the functional effect of phosphorylation of these three RyR2 residues; however, intracellular Ca^{2+} imaging, when hyperphosphorylated at Serine 2808, shows Ca^{2+} leak (Fischer *et al.*, 2015). It is proposed that hyperphosphorylation of the RyR2 can result in a reduction in the release threshold, causing SOICR events, which is linked to arrhythmias (Xiao *et al.*, 2007). Because many kinases phosphorylate serine/threonine residues, an abundance of serine and threonine residues within RyR2 make it plausible to assume that there may be many other kinases and phosphorylation sites that could affect the activity of RyR2.

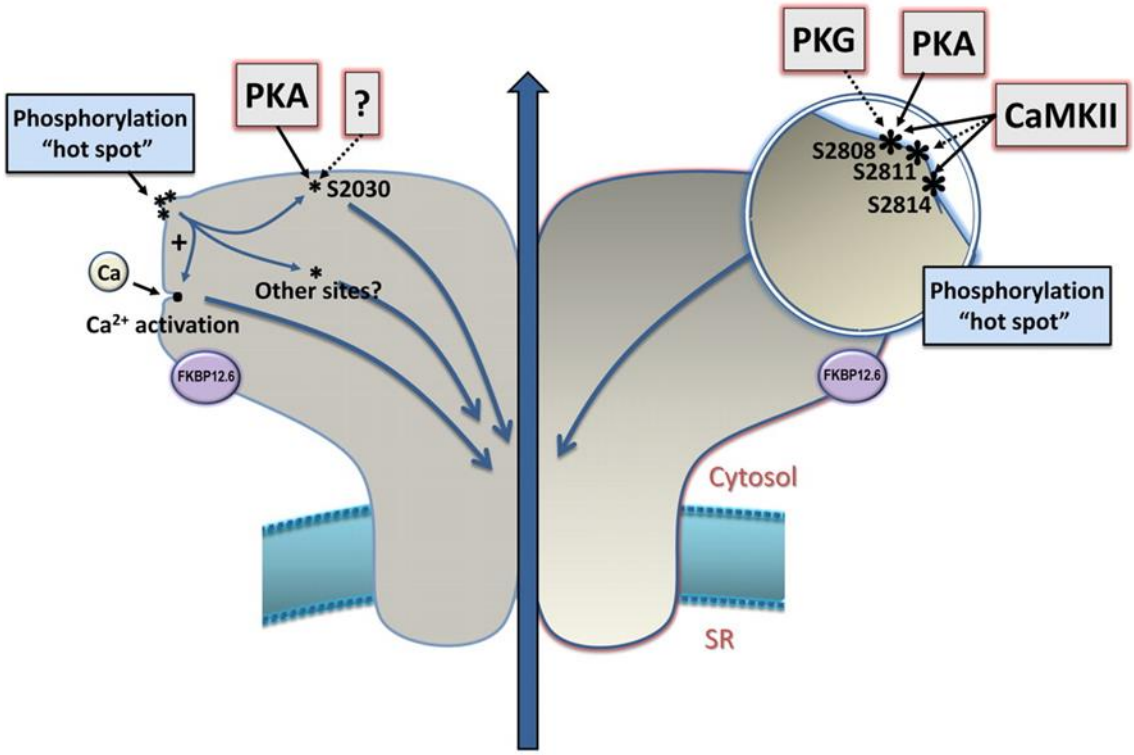

Figure 1.4 RyR2 – Multi-phosphorylation Site Model.
Proposed model of RyR2 showing a specific phosphorylation "hot spot". Within this "hot spot" serine 2808, 2811 and 2814 are proposed to be able to be phosphorylated by PKA and CaMKII. Image taken from (Valdivia, 2012).

As mentioned, pathophysiological conditions can result in an increased activity of kinases including CaMKII and PKA. Acute hyperglycemic environments have shown to cause the addition of O-linked glycosylation at the serine 279 region of CaMKII (Erickson *et al.*, 2013).

This O-linked glycosylation modification of CaMKII results in overactivation of the kinase, leading to spontaneous Ca^{2+} release from the SR, which had been also linked with arrhythmogenesis (Erickson *et al.*, 2013). Similarly, the hyperglycaemic environment in DM increases the production of diacylglycerol (DAG) an agonist for protein kinase C (PKC) (Xia *et al.*, 1994). PKC and protein kinase G (PKG) are two other kinases that have been shown to be able to phosphorylate the RyR2, although their effect and the residues targeted are unknown (Takasago *et al.*, 1991).

1.4 PKC

PKC is a family of kinases that can regulate the activity of proteins via phosphorylation of hydroxyl groups on serine or threonine amino acid residues (Newton, 2003). The PKC family contains 15 different isoforms within humans, all of which are divided into 3 separate subfamilies based on their activation requirements; conventional (cPKC), novel (nPKC) and atypical (aPKC) (Newton, 2003). PKC's function has been well described in cell proliferation, cell survival and cell apoptosis, where changes in PKC expression have been linked to many diseases including cancer, Alzheimer's disease and DM (Hongpaisan *et al.*, 2011; Liao *et al.*, 2013; Maurya & Vinayak, 2015). In the heart, PKC has been shown to be involved in myocardial infarction, acute reperfusion injury, compensatory hypertrophy and vascular dysfunction (Braz *et al.*, 2004; Mochly-Rosen *et al.*, 2012; Newton *et al.*, 2016). Western blot analysis shows that within a rat heart, PKC isoforms; α, β_2, δ, ε and γ are expressed, with PKCα as the most expressed isozyme in the human heart (Borghini *et al.*, 1994; Ping *et al.*, 1997; Simonis *et al.*, 2007; Geraldes & King, 2010).

1.4.1 Structure of PKC

All PKC isoforms contain a regulatory domain connected to a catalytic domain via a hinge region (Geraldes & King, 2010; Steinberg, 2012). Among all three subfamilies of PKC, the catalytic domain is conserved (Geraldes & King, 2010; Steinberg, 2012). The catalytic domain contains a C3 region, specific for ATP binding and a C4 region, for substrate binding (Figure 1.5) (Geraldes & King, 2010; Steinberg, 2012). Within the regulatory domain is a pseudosubstrate region, which contains a small amino acid sequence that binds and inhibits the catalytic domain (Geraldes & King, 2010; Steinberg, 2012). The subfamilies differ in the regulatory domain. cPKC and the nPKC subfamilies contain a C1 region within the regulatory domain, for the binding of DAG (Figure 1.5) (Geraldes & King, 2010). cPKC is the only subfamily with a C2 region that has a Ca^{2+} binding/sensor (Figure 1.5) (Geraldes & King, 2010).

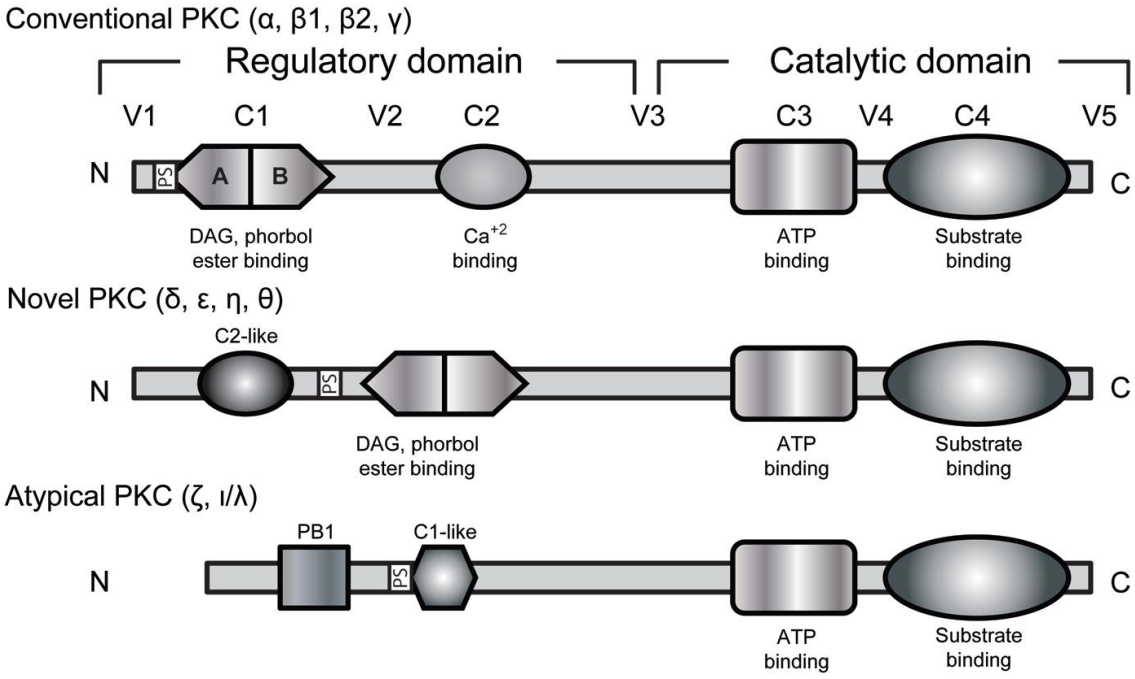

Figure 1.5 Structure of PKC isoforms.
cPKC, nPKC, and aPKC contain a regulatory domain connected to the catalytic domain via the hinge region. In cPKC's, the regulatory domain contains a C1 region for DAG binding and a C2 region for Ca^{2+} binding to activation of the kinase. In nPKC's, the regulatory domain contains a C1 region for DAG binding for activation of the kinase. In aPKC's, the regulatory domain contains a PB1 region for phosphatidylinositols binding for activation of the kinase. The catalytic domain containing a C3, ATP binding region and a C4, substrate binding region. Pseudosubstrate within the regulatory domain region inhibits the catalytic domain in all 3 sub-classes. Image taken from (Geraldes & King, 2010).

1.4.2 Activation of PKC

cPKC's and nPKC's can both be activated by G-protein coupled receptor αq (GPCR-αq) activation (Figure 1.6) (New & Wong, 2007). When the correct ligand binds to this GPCR-αq, GDP bound on the alpha subunit is dissociated with GTP, resulting in the dissociation and activation of the alpha, beta and gamma subunits (Figure 1.6) (Kamato *et al.*, 2017). The alpha subunit then activates phospholipase-C (PLC) on the plasma membrane of the cell (Figure 1.6) (Kamato *et al.*, 2017). PLC cleaves Inositol Phospholipids (PIP2) into DAG and inositol 1,4,5-triphosphate (IP3) (Figure 1.6) (Kamato *et al.*, 2017). IP3 then activates IP3-gated Ca^{2+} channels on the SR, resulting in Ca^{2+} release (Figure 1.6) (Kania *et al.*, 2017). Under basal conditions, the pseudosubstrate sequence binds the C4 region keeping the enzyme inactive (Kirwan *et al.*, 2003). In cPKC's, Ca^{2+} binds to Ca^{2+} binding residues within the C2 region of the regulatory domain allowing for the translocation of the kinase to the cell membrane (Eshete *et al.*, 1998). However, in nPKC's, the C2 region lacks Ca^{2+} binding residues and therefore is translocated to the membrane in a Ca^{2+} independent manner (Zhang & Aravind, 2010). At the cell membrane, DAG binds at the C1 region of the regulatory domain, resulting in the removal of the pseudosubstrate from the C4 region, thus activating the kinase (Kirwan *et al.*, 2003). aPKC's are activated by phosphatidylinositol's such as phosphatidylinositol (3,4,5)-trisphosphate (PIP3) along with protein-protein interaction between pyruvate dehydrogenase kinase 1 (PDK1) (Xiao & Liu, 2013).

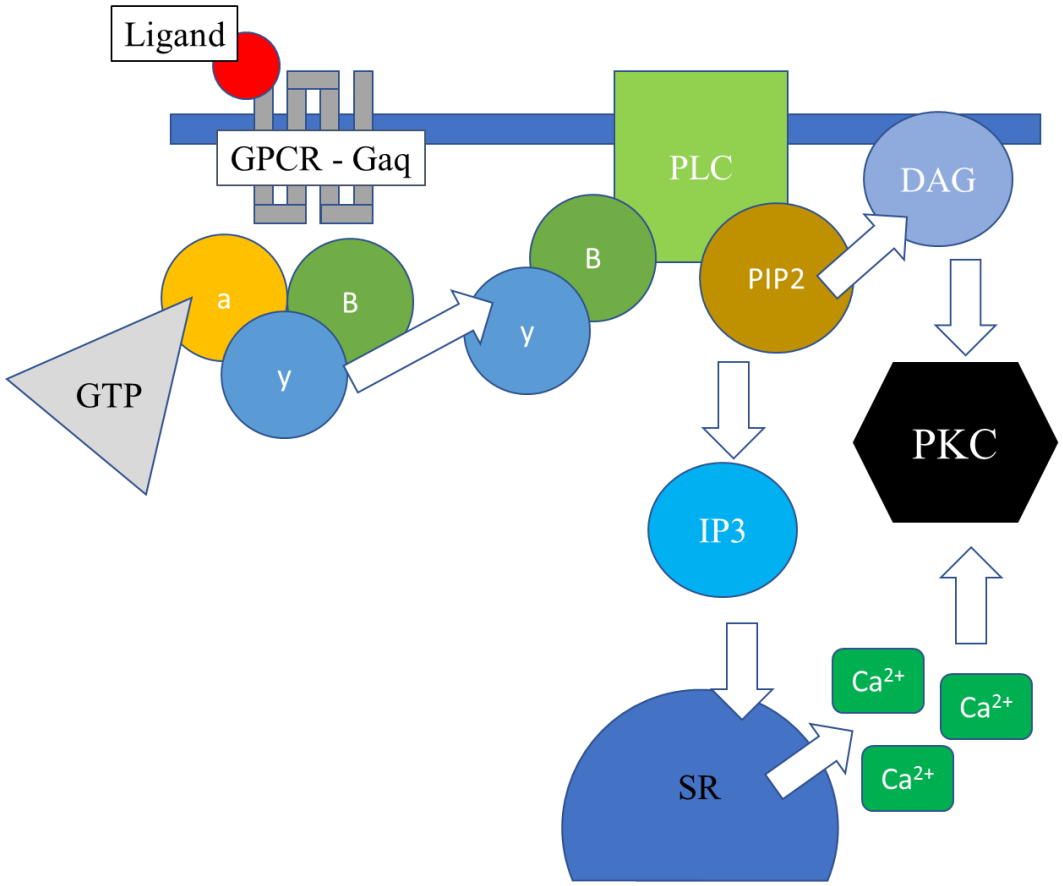

Figure 1.6 Activation of PKC through GPCR.
Binding of a ligand results in a downstream pathway resulting in activation of PLC which cleaves PIP2 into IP3 and DAG. IP3 then causes Ca^{2+} release from the SR. Ca^{2+} allows for the translocation of cPKC to the PM to interact with DAG for activation. DAG alone can activate nPKC. Created with Microsoft PowerPoint.

1.4.3 PKC Activity in Diabetes

The chronic hyperglycaemic environments seen in DM results in many molecular and biochemical changes which underlie the multitude of pathologies associated with DM. In normal physiological states, many proteins/lipids are glycosylated, with the covalent bonding of sugar molecules added to them with enzymatic control (Aebi, 2013). However, hyperglycemic environments can result in glycation, covalent bonding of sugar molecules to proteins and lipids without enzymatic function within hours (Adrover *et al.*, 2008). These glycated proteins/lipids (Schiff bases) can then be turned into Amadori products if the hyperglycaemic environment persists, both of which are reversible using glycaemic control (Figure 1.7) (Pieters *et al.*, 2007). Within weeks or months of chronic hyperglycaemic

environments, as seen in DM, Amadori products then become irreversible advanced glycated end products (AGE's) (Figure 1.7) (Stitt *et al.*, 1998). AGE's can then result in pathophysiological changes resulting in inflammation, oxidative stress, and fibrosis which are linked to vascular dysfunction (Bodiga *et al.*, 2014). Schiff bases, as well as Amadori products, can also lead to reactive intermediates (Figure 1.7) (Puttaiah *et al.*, 2006). These reactive intermediates can then result in many physiological changes including increasing the synthesis of DAG (Xia *et al.*, 1994). In the DM rat heart, PKC isoforms α, ε, β_2 and δ have an increased activity, however, the consequence of each individual isoform is not well understood (Geraldes & King, 2010).

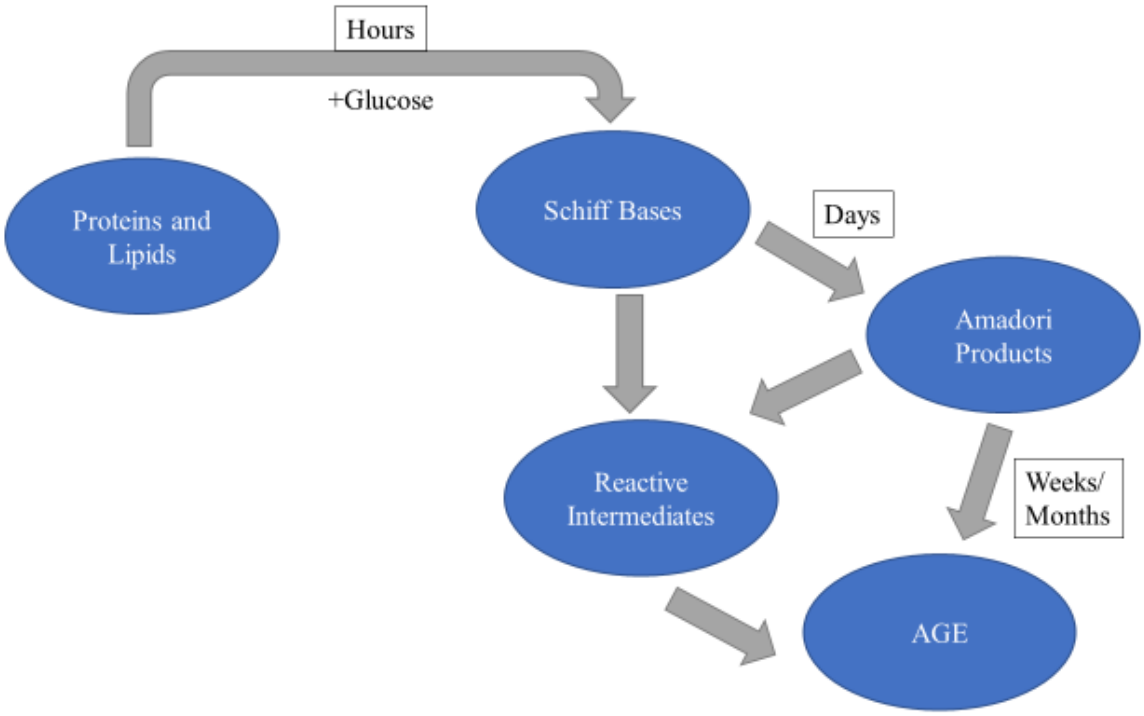

Figure 1.7 Formation of AGE's
Glycation of proteins and lipids in the presence of glucose form Schiff bases. Within Weeks/Months, there is a build of reactive intermediates and AGEs seen in DM. It is the reactive intermediates that result in an increase in DAG in DM patients. Created with Microsoft PowerPoint.

1.5 Aims and Hypothesis

DM leads to many forms of molecular and biochemical changes which can result in post-translational modification of proteins in the heart, including phosphorylation, oxidation, and glycation, which may explain the links between DM and CVD (Bodiga *et al.*, 2014). As described in Section 1.4.3, hyperglycemic environments have been shown to cause an accumulation in DAG due to increased glycolytic intermediates, which then results in an increased activation of PKC, which has been associated with many vascular alterations including diabetic neuropathy (Geraldes & King, 2010). The molecular pathways through which DM has an increased risk or association to arrhythmia is not fully understood. It is well described that phosphorylation of RyR2 can result in SOICR, however, the effect of PKC phosphorylation on RyR2 and the occurrence of SOICR has not yet been investigated. Research investigating how an increase in PKC activation or expression, as seen in DM, can affect the RyR2 resulting in SOICR could serve as the molecular pathway linking DM and arrhythmia.

Therefore, the aim of the study is to assess the effect of PKC on the occurrence of SOICR and the store dynamics of Ca^{2+} release. To test the aim, I will complete the following objectives:

1. The effect of endogenous PKC on SOICR
2. The effect of PKCα on SOICR and store dynamics
3. The effect of PKCε on SOICR and store dynamics

I hypothesise that activation and inhibition of endogenous PKC would result in an increase and decrease in the occurrence of SOICR respectively. I also hypothesise that both overexpression of PKCα and PKCε will increase the occurrence of SOICR due to a decrease in the release threshold of the SR.

2 Methods

2.1 Cell Culture

2.1.1 Preparation of HEK293 Cells for Subculture

Flp-In T-REx human embryonic kidney 293 (HEK293) cells expressing RyR2 under the control of the tetracycline repressor were stored in at minus 80 °C. A 1 mL aliquot of thawed HEK293 cells were added to a 75 cm^2 culture flask containing 30 mL of pre-warmed (37°C) Dulbecco's Modified Eagle's Medium (DMEM) solution (1.8 mM $CaCl_2$, 25 mM D-Glucose, 5.3 mM KCL, 4 mM L-Glutamine, 0.8 mM $MgSO_4$, 110 mM NaCl, 33 mM $NaHCO_2$, 0.9 mM NaH_2PO-H_2O – pH 7.4) modified with 10% fetal bovine serum (FBS), 1% non-essential amino acids (NEAA), 1% penicillin and 1% streptomycin. HEK293 cells were then cultivated in a humidified incubator, maintained at 37 °C with an atmosphere of 5% CO_2. After 24 hours of cultivation, the existing growth medium was aspirated and replaced with 20 mL of fresh pre-warmed (37 °C) DMEM solution.

2.1.2 Subculture

Once HEK293 cells in 75 cm^2 or 25 cm^2 culture flasks reached the desired confluence (~90%), they were then re-subcultured into either a 75 cm^2 or 25 cm^2 culture flask, where a maximum of nine passages was allowed before HEK293 cells were discarded and a new batch of HEK293 cells were subcultured. First, the existing growth medium was aspirated and cells were washed twice with either 5 mL or 2 mL of pre-warmed sterile phosphate buffered saline (PBS) (2.7 mM KCL, 1.8 mM KH_2PO_4, 137 mM NaCl, 10 mM Na_2HPO_4 – pH 7.4), followed by a 5-minute incubation in either 3mL or 1mL PBS at room temperature (22 - 25 °C), depending on the culture flask size (75 cm^2 or 25 cm^2 respectively). The cell culture flask was then agitated to allow for detachment of the HEK293 cells from the internal surface. 17 mL or 6.5 mL of fresh

pre-warmed DMEM solution was added, respective to the culture flask size; 75 cm^2 or 25 cm^2, to attain a final volume of 7.5 mL or 20 mL. The mixture was then pipetted 3 times to ensure homogenous cell suspension. HEK293 cells from the 25 cm^2 culture flask were then seeded onto glass coverslips for single-cell imaging or into another culture flask for later use. HEK293 cells that were transferred into new 25 cm^2 culture flask were diluted with fresh pre-warmed DMEM, with the volume determined by the required time of incubation. HEK293 cells from the 75 cm^2 culture flask could then be transferred into 100 mm diameter cell culture dishes in preparation for cell lysate collection or subcultured into another culture flask for later use. Cell proliferation of HEK293 cells was maintained for 24-72 hours before cells were used for single-cell imaging or the preparation of cell lysate collection for western blot analysis. An inverted microscope was used to assess cell confluence, and confirm the absence of bacterial or fungal contaminants.

2.1.3 Preparation of HEK293 Cells for Imaging

In preparation for single-cell imaging (Section 2.2), 13 mm diameter glass coverslips were sterilized in 70% ethanol and placed into a six-well culture plate (three glass coverslips per well). The coverslips were coated with poly-L-lysine for 5 minutes to facilitate cell adhesion. 1 mL of suspended HEK293 cells from the 25 cm^2 culture flask (Section 2.1.2) was then diluted in 18 mL of fresh pre-warmed (37 °C) DMEM, followed by an aliquot of 3 mL per well. In preparation of cell lysate collection for western blot analysis (Section 2.3), 1 mL of suspended HEK293 cells from the 75 cm^2 culture flask (2.1.2) was added to each 100 mm diameter cell culture dishes containing 9 mL of fresh pre-warmed DMEM.

2.1.4 HEK293 cDNA Transfection

HEK293 cells were transfected using the Ca^{2+}-phosphate precipitation method which facilitates the endocytosis of cDNA into the cells (Graham & van der Eb, 1973). A 500 µL $CaCl_2$-cDNA (62 µL $CaCl_2$ + 5 µg cDNA + ddH_2O to make 500 µL) transfection mixture was pipetted in a dropwise motion into a separate 50 mL tube containing 500 µL HEPES buffered saline (1.2 mM $CaCl_2$, 20 mM HEPES, 2.4 mM K_2HPO_4, 1.2 mM $MgCl_2$, 115 mM NaCl – pH 7.4) where agitation of the solution was required to ensure co-precipitation. Thereafter, co-precipitate containing 0.9 µg of cDNA was then added into the individual wells of the culture plates 24 hours post-seeding of the HEK293 cells (Section 2.1.3). For cytosolic Ca^{2+} imaging (Section 2.2.1), individual wells were either transfected with or without PKCα/ε cDNA. Specifically, for luminal Ca^{2+} imaging (Section 2.2.2), 5 µg of D1ER cDNA was also included in the transfection mixture for each condition. For lysate collection (2.3.1), 5µg PKCα cDNA or mock (cDNA excluded) was added to each cell culture plates, 24 hours post-preparation of HEK293 cells (Section 2.1.3).

2.1.5 Induction of RyR2 Expression

Twenty-four hours post-transfection (Section 2.1.4) of HEK293 cells grown on 13 mm diameter glass coverslips for single-cell imaging, the existing growth medium was aspirated and each well was washed twice with 3 mL of pre-warmed DMEM. For cytosolic Ca^{2+} imaging (Section 2.2.1), HEK293 cells were induced with 0.1 µg of tetracycline to induce RyR2 expression per well. For luminal Ca^{2+} imaging (Section 2.2.2), HEK293 cells were induced with 0.3 µg of tetracycline per well. HEK293 cells grown in 100 mm diameter culture plates for the collection of cell lysates (Section 2.3.1), were induced with 10 µg of tetracycline per plate.

2.2 Single-cell Imaging

2.2.1 Cytosolic Ca^{2+} Imaging

To assess SOICR, HEK293 cells grown on glass coverslips, transfected with or without PKCα/ε were imaged 16-20 hours post-induction (Section 2.1.5). The acetoxymethyl ester (AM) form of the Ca^{2+} indicator, Fluo-4 AM dissolved in dimethyl sulphoxide (DMSO) and 12% pluronic acid enabled the visualisation of Ca^{2+} release events, known as SOICR. Glass coverslips were rinsed in 0 mM Ca^{2+} Krebs-ringer HEPES (KRH) (25 mM HEPES, 125 mM NaCl, 6 mM Glucose, 5 mM KCL, 1.2 mM $MgCl_2$ – pH 7.4) followed by an incubation in 1 mL of Ca^{2+} free KRH containing 1 mg/mL of bovine serum albumin (BSA) with 2.5 µM Fluo-4 AM solution for 10 minutes, followed by a 10-minute wash in 0 mM Ca^{2+} KRH, before being mounted on the perfusion chamber. Coverslips were imaged on an inverted microscope with a 20x objective lens while being superfused with KRH containing incremental Ca^{2+} concentrations (0, 0.1, 0.2, 0.3, 0.5, 1 mM), followed by 1 mM Ca^{2+} + 20 mM caffeine (RyR2 agonist) for the duration of 2, 4, 4, 4, 4, 4 and 2 minutes respectively (Kong *et al.*, 2008). Caffeine was used to confirm RyR2 expression in each cell. The flow of the solutions was driven by gravity with a constant superfusion flow rate of ~3 mL per minute. The initial raw data collected was a video recording of HEK293 cells, within a chosen field of view, over the 24 minute experimental time course using NIS-Elements AR software (v4.0). The region of interest on the coverslip was determined using light microscopy to find an area of well distributed and appropriately confluent cells. The Fluo4-AM loaded in HEK293 cells underwent excitation at 470 nm with emission captured through a long-pass emission filter (>515 nm) with an exposure time of 100 milliseconds, while images were collected every 2 seconds. A separate region of interest (ROI) was drawn around 150-250 cells per glass coverslip and the SOICR events were seen as transient increases cytosolic Ca^{2+} (fluorescence peaks).

2.2.1.1 Data Analysis

The susceptibility to SOICR was determined by the Ca^{2+} concentration required to elicit the initial occurrence of fluorescent peaks. Traces of cytosolic Ca^{2+} fluorescence are presented as F/F_0, with F indicative of the fluorescent intensity at time point, t, and F_0 indicative of the fluorescent intensity recorded at 0 mM Ca^{2+}. The cumulative fraction of cells experiencing SOICR at each Ca^{2+} concentration was then calculated and fitted with a non-linear regression for the individual glass coverslip, where the sample size (n) is the number of coverslips per condition. Cells that experienced SOICR events at 0 mM Ca^{2+} were excluded as they represent unhealthy cells. Cells that had no caffeine-induced Ca^{2+} transients at 1 mM Ca^{2+} with 20 mM caffeine were also excluded, as changes in fluorescent intensity could not be attributed to RyR2 mediated release.

2.2.2 Luminal Ca^{2+} Imaging

To assess the characteristics of SOICR, HEK293 cells grown on glass coverslips that were transfected with D1ER, with or without co-transfection of PKCα/ε were imaged 16-20 hours post-induction. Glass coverslips were washed in 0 mM Ca^{2+} KRH for 10 minutes before being mounted on the perfusion chamber. Coverslips were imaged on an inverted microscope with a 20 x objective lens while being superfused with KRH containing 0 mM Ca^{2+}, 1 mM Ca^{2+}, 2 mM Ca^{2+}, 2 mM Ca^{2+} + 2 mM tetracaine and 2 mM Ca^{2+} + 20 mM caffeine for the duration of 2, 4, 7, 5 and 5 minutes respectively. 1-2 mM Ca^{2+} results in oscillations of fluorescence, where the downward peak represents Ca^{2+} release through RyR2 from the SR, while the upward peak is Ca^{2+} filling into the SR via SERCA. As the amount of Ca^{2+} load within the SR is dependent on the balance of SERCA-mediated influx and RyR2-mediated efflux, inactivation of RyR2 renders the amount of Ca^{2+} load dependant on SERCA. Therefore, tetracaine, a RyR2 antagonist, results in an upward peak of fluorescence due to Ca^{2+} filling the SR to the maximum (Overend *et al.,* 1997). Caffeine, a RyR2 agonist, results in a downward peak of fluorescence

is due to complete depletion of Ca^{2+} through RyR2 from the SR (Kong *et al.*, 2008). The flow of the solutions was driven by gravity with a constant superfusion flow rate of ~3 mL per minute. As described in Section 2.2.1.1, data of cells fluorescing over the 24 minute experimental time course were collected by NIS-Elements AR software (v4.0). D1ER underwent excitation at 436 nm with emissions of the yellow fluorescent protein (YFP) and cyan fluorescent protein (CFP) captured through a dual dichronic beamsplitter at 535 nm and 480 nm respectively with an exposure time of 100 milliseconds. The two image recordings of the YFP and CFP channel were collected simultaneously every 2 seconds, where the amount of fluorescence resonance energy transfer (F) was determined by the ratio of these emissions (YFP/CFP). A ROI was drawn around 10-40 cells per glass coverslip.

2.2.2.1 Data Analysis

Four parameters were derived from the traces of luminal Ca^{2+} fluorescence for each cell, as shown in Figure 2.1; F_{max}, F_{min}, F_{SOICR}, and F_{termi}. Between 0-2 mM Ca^{2+}, oscillations of F represent the release of Ca^{2+} through the RyR2 from the SR (downward deflection) and the refilling of Ca^{2+} into the SR through SERCA activity (upward deflection). The average peaks of oscillation represent the luminal Ca^{2+} required to activate RyR2 Ca^{2+} release, termed the release threshold of SOICR (F_{SOICR}), where the average nadir of oscillation represents the luminal Ca^{2+} required to inactivate RyR2 Ca^{2+} release and is termed the termination threshold (F_{termi}) of SOICR. As described in Section 2.2.2, the subsequent addition of tetracaine and caffeine determined the maximum (F_{max}) and minimum (F_{min}) capacity of SR Ca^{2+} store, respectively. These parameters were normalised to F_{min}, and the characteristics of SOICR were calculated; store size ($F_{max} - F_{min}$), release threshold ($[F_{SOICR} - F_{min}] / [F_{max} - F_{min}] \times 100$), termination threshold ($[F_{termi} - F_{min}] / [F_{max} - F_{min}] \times 100$). The percentage of store size, release threshold and termination threshold of cells were then calculated and plotted, where the sample size (n) is the number of cells per condition.

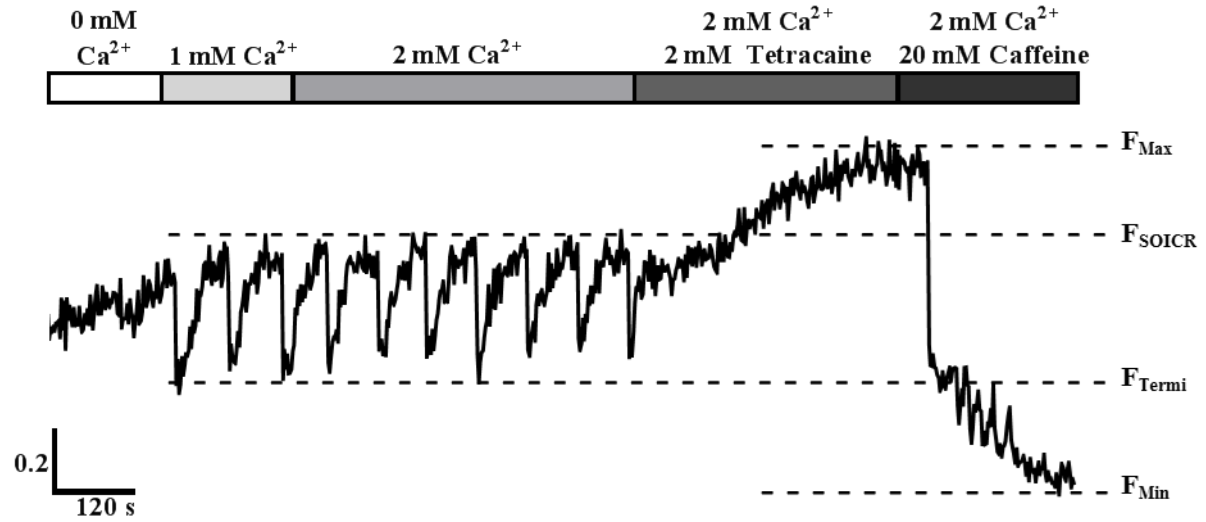

Figure 2.1 Luminal Ca^{2+} Fluorescent Trace.
The parameters used to determine the characteristics of SOICR; maximum (F_{max}), minimum (F_{min}), release threshold (F_{SOICR}) and termination threshold (F_{termi}). Bar represents the concentration of the superfusate, and the length of the bar is proportional to the duration of superfusion.

2.3 Western Blot

2.3.1 Collection of HEK293 Cell Lysates

HEK293 cells were grown in ten 100 mm diameter culture dishes for each condition (Section 2.1.2). After 24 hours, the culture plates were either transfected with or without PKCa cDNA (Section 2.1.4). 24 hours post-transfection, the plates were then induced undiluted tetracycline (Section 2.1.5), 18 hours prior to harvesting of HEK293 cells. Growth medium was discarded and culture dishes were washed twice in PBS containing 0.5 mM ethylenediaminetetraacetic acid (EDTA) then incubated with 2.5 mL of PBS-EDTA for 10 minutes. Plates were agitated to allow the detachment of HEK293 cells from the internal surface. PBS-EDTA solution containing HEK293 cells was collected into a 50 mL tube, where a further 1.25 mL of PBS-EDTA solution was added to each plate for the collection of any residual cells, making a total of 37.5 mL per condition. Tubes containing cells were centrifuged at 1000 g for 10 minutes. The supernatant was discarded and the pellet was resuspended with 2 mL of lysis buffer (1% CHAPS, 25 mM HEPES/Tris, 137 mM NaCl, 0.5% Soybean phosphatidylcholine – pH 7.05)

containing protease inhibitors (2 µg/ml Aprotinin, 1 Mm Benzamide, 2.5 mM DTT, 2 µg/ml Leupeptin, 2 µg/ml Pepstatin A, 0.525 mM PMSF) to minimise protein degradation for 1 hour on ice. To remove insoluble material, lysates were separated into two 1 mL eppendorff tubes and centrifuged at 16,000 g for 30 minutes at 4 °C, where the supernatant was then transferred into two CyroTubes and cryopreserved at minus 80 °C until required for sodium dodecyl sulfate (SDS) polyacrylamide gel electrophoresis (SDS-PAGE) (Section 2.3.4). The protein concentration was measured on a BioTek Take3 Micro-Volume Plate Reader, where for each condition, 3 biological samples were conducted.

2.3.2 Preparation of Polyacrylamide Gels

Two glass plates pre-cleaned with 70% ethanol were loaded onto a plastic clamp to form a gel cast. Running gel solution was pipetted to fill approximately 70% of the gel cast, this was overlaid with 1 mL of H_2O to prevent gel desiccation. Running gel was left to set at room temperature for 1-hour. A 6% and 12% acrylamide running gel was made for total RyR2 and total PKCα with glyceraldehyde 3-phosphate dehydrogenase (GAPDH) respectively. Once the gel had set, the H_2O was removed and stacking gel solution was pipetted to fill the rest of the gel cast. While ensuring for no air bubbles, a 10 well plastic gel comb, with 1.5 mm wells, was introduced for the formation of wells and the gel was left to set at room temperature for 1 hour for the formation of a polyacrylamide gel.

Table 2.1 Running Gel

Ingredients	**6%** **(µL)**	**12%** **(µL)**
MilliQ-H_2O	4632	3432
Tris/ HCl (1.5 M - pH 8.8)	2000	2000
Acrylamide (40%)	1200	2400
SDS (10%)	80	80
APS (Ammonium persulfate) (10%)	80	80
TEMED (Tetramethylethylenediamine)	8	8

Table 2.2 Stacking Gel

Ingredients	**4%** **(µL)**
MilliQ-H_2O	5032
Tris/ HCl (0.5 M - pH 6.8)	2000
Acrylamide (40%)	800
SDS (10%)	80
APS (10%)	80
TEMED	8

2.3.3 Sample Preparation for SDS-PAGE

Cell lysates were thawed and diluted with an appropriate volume of Laemmli's sample buffer (SB) (10% β-mercaptoethanol, 0.004% Bromphenol Blue, 20% Glycerol, 4% SDS, 125 µM Tris-HCl). Samples were solubilised in a heating block at 95 °C for 7 minutes to denature the proteins and centrifuged at 1400 g for 2 minutes to remove insoluble material.

2.3.4 SDS-PAGE

SDS-PAGE was used to separate protein based on its molecular weight. The gel cassette containing the gel (Section 2.3.2) was introduced into the electrophoresis tank filled with running buffer (192 mM Glycine, 0.1% SDS, 25 mM Tris). The plastic comb was removed carefully from the gel where prepared samples containing 3µg/µL of protein (Section 2.3.3) were loaded from left to right after the addition of 7 µL of Precision Plus Protein Ladder in the first well to visualise protein migration; sample order was: Ladder, Mock #1, PKCα #1, Mock #2, PKCα #2, Mock #3 and PKCα #3. SDS-PAGE ran for 1-hour at 60 V, 400 mA to allow the samples to move through the stacking gel. The voltage was then turned up to 100V and left for 4 or 1 hours for the 6% and 12% gel respectively.

2.3.5 Membrane Transfer

A wet-transfer method was used to transfer proteins to a nitrocellulose membrane. The gel was detached carefully from the cassette, removing the stacking gel layer before being placed within a transfer sandwich (sponge, filter paper, nitrocellulose membrane, gel, filter paper, sponge) held together by a transfer cassette. The transfer cassette was then introduced into a transfer tank filled with transfer buffer (192 mM Glycine, 20% Methanol, 0.01% SDS, 25 mM Tris). The protein samples were transferred from the gel to the nitrocellulose membrane overnight (900 minutes) in a 4 °C room, set at 54 V, 400 mA.

2.3.6 Membrane Blotting

The membrane was removed from the transfer sandwich and placed in a container with Ponceau S total protein stain to check for clear band transfer to the membrane. The membrane was then washed in PBS, followed by two PBS with 0.5% tween-20 (PBS-T) washes. The membrane containing PKCα and GAPDH protein from the 12% gel was then cut into two separate membranes at the 50 kDa ladder band to allow the processing of the proteins independently. The membranes were then incubated in a 5% milk PBS-T solution for 1.5 hours to prevent non-specific antibody binding, where all incubations occurred on a platform mixer unless stated otherwise. The membranes were then washed with PBS three times, ensuring complete removal of the milk PBS-T solution before being incubated with a primary antibody. The membrane containing RyR2 from the 6% gel was incubated in mouse-anti-RyR2 (Abcam, 1: 1,000 dilution) for 4 hours. The membrane containing PKCα from the 12% gel was incubated in mouse-anti-PKCα (Abcam, 1: 1,000 dilution) for 2 hours. The membrane containing GAPDH was incubated in rabbit-anti-GAPDH conjugated with horseradish peroxidase (HRP) (Abcam, 1: 2,500 dilution) for 2 hours. The membranes were then washed with PBS-T three times (5 minutes, 10 minutes, 5 minutes) followed by three PBS washes. Membranes containing RyR2 as well as PKCα were then incubated separately with the same HRP conjugated secondary antibodies, goat-anti-mouse (Abcam, 1: 20,000 dilution) for 2 hours, then washed with PBS-T three times (5 minutes, 10 minutes, 5 minutes) followed by three PBS washes.

2.3.7 Membrane Developing

Membranes were incubated in 4 mL of Super Signal West Pico Chemiluminescent Substrate for 5 minutes while tilting the box. The membrane was then placed between two clear plastic sheets and images were captured in Syngene Pxi 4 Imager.

2.3.8 Western blot analysis

Densitometry analysis was performed with GeneTools (v4.0) software, normalised to GAPDH ([Density of RyR2 or PKCα] / [Density of GAPDH from the same sample]). The data was then processed to give the fold change of PKCα transfected HEK293 cells to mock transfected HEK293 cells for both total RyR2 and PKCα ([normalised PKCα or Mock transfection density] / [Mock transfection density average]).

2.4 Statistical Analysis

All statistical analyses were performed on GraphPad Prism (v6.0) software, where statistical significance is denoted as $p \leq 0.05$ *, $p \leq 0.01$ **, $p \leq 0.001$ ***, data are expressed as mean ± standard error of the mean (SEM). For data sets that presented a normal distribution; western blot analysis and luminal Ca^{2+} imaging analysis, an unpaired two-tailed student's t-test was used. For data sets that contained more than two conditions including; luminal Ca^{2+} imaging, a one-way analysis of variance (ANOVA) was performed. For data sets that contained two variables with more than two conditions including; cytosolic Ca^{2+} imaging analysis, a two-way ANOVA was performed along with the most appropriate post-hoc test, mentioned for each result (Dunnett or Sidak).

.

3 Results

3.1 Cell Viability

Before using the HEK293 cells they were first examined under a microscope to check cell health and density. Light microscopy was used to confirm the confluence of the HEK293 cells and to examine for bacterial or fungal contamination. An inverted microscope was used to confirm the uptake of the cytosolic Ca^{2+} indicator dye, Fluo-4 AM into the HEK293 cells prior to cytosolic Ca^{2+} imaging and to confirm the transfection of the luminal Ca^{2+} indicator protein, D1ER prior to luminal Ca^{2+} imaging. Figure 3.1 A shows a non-contaminated and well-distributed view of HEK293 cells. Figure 3.1 B shows uptake of Fluo-4 AM while Figure 3.1 C shows transfection of D1ER protein. For D1ER note the reticular pattern indicating expression within the Ca^{2+} store lumen.

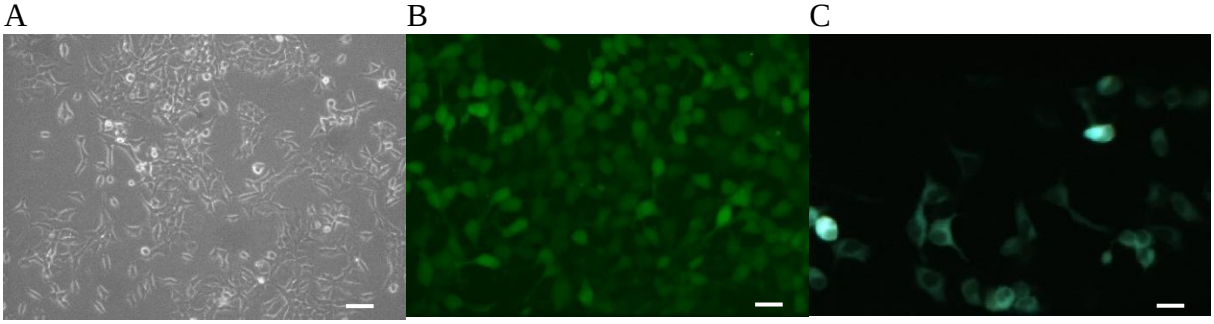

Figure 3.1 HEK293 Cells Visualised Using Microscopy.
(A) Non-contaminated, well distributed HEK293 cells. (B) Successful loading of Fluo-4 AM into HEK293 cells. (C) Successful D1ER transfection in HEK293 cells. Scale bar 50µm.

3.2 Endogenous PKC

3.2.1 Cytosolic Ca^{2+} Imaging

3.2.1.1 Endogenous PKC Activation

In DM, there is an increase in the accumulation and synthesis of DAG resulting in increased PKC activity. To mimic this effect in HEK293 cells, the PKC activator 1,2-dioctanoyl-sn-glycerol (Dic8), a DAG analogue, was used to activate endogenous PKC (Stahelin et al., 2005).

See Figure 3.4 for endogenous PKC expression level quantification. HEK293 cells were loaded with the cytosolic Ca^{2+} indicator dye, Fluo-4 AM and continuously superfused with KRH containing increasing Ca^{2+} concentrations (0, 0.1, 0.2, 0.3, 0.5, 1 mM) to elicit SOICR. To confirm RyR2 expression the HEK293 cells were superfused with 1 mM Ca^{2+} KRH solution containing 20 mM caffeine at the end of each experiment. Caffeine is a RyR2 agonist and depletes the luminal Ca^{2+} store which can be observed as a large increase in cytosolic Ca^{2+}. SOICR events were visualised as transient peaks in the cytosolic Ca^{2+} fluorescence as seen in Figure 3.2 A. The cumulative fraction of cells in each condition (Vehicle treated, 10 µM Dic8 treated and 20 µM Dic8 treated HEK293 cells) exhibiting Ca^{2+} oscillations (SOICR events) was plotted against the concentration of Ca^{2+}. These data points were fitted with a non-linear regression (Vehicle treated HEK293 cells $R^2 = 0.87$, 10 µM Dic8 treated HEK293 cells $R^2 = 0.90$ and 20 µM Dic8 treated HEK293 cells $R^2 = 0.84$) and statistical significance assessed with a two-way ANOVA with a Dunnett's post hoc test. As shown in Figure 3.2 B, an increase in Ca^{2+} concentration in the superfusate resulted in an increase in the fraction of cells undergoing SOICR in a dose-response manner for each condition as expected. The addition of 10µM Dic8 resulted in an increase in the percentage of cells undergoing SOICR compared to the vehicle treated HEK293 cells at 0.3 mM Ca^{2+} (47.69 ± 3.7 versus 34.85 ± 4.0) ($p = 0.013$). Application of 20 µM Dic8 led to a greater increase in the percentage of cells undergoing SOICR compared to the vehicle treated HEK293 cells at 0.2 (30.07 ± 13.11 versus 16.82 ± 3.38) ($p = 0.046$), 0.3 (52.37 ± 9.27 versus 34.85 ± 4.0) ($p = 0.006$), 0.5 (67.23 ± 4.79 versus 51.32 ± 2.93) ($p = 0.014$) and 1 mM Ca^{2+} (77.7 ± 4.07 versus 63.31 ± 2.56) ($p = 0.028$) suggesting a dose response effect.

A

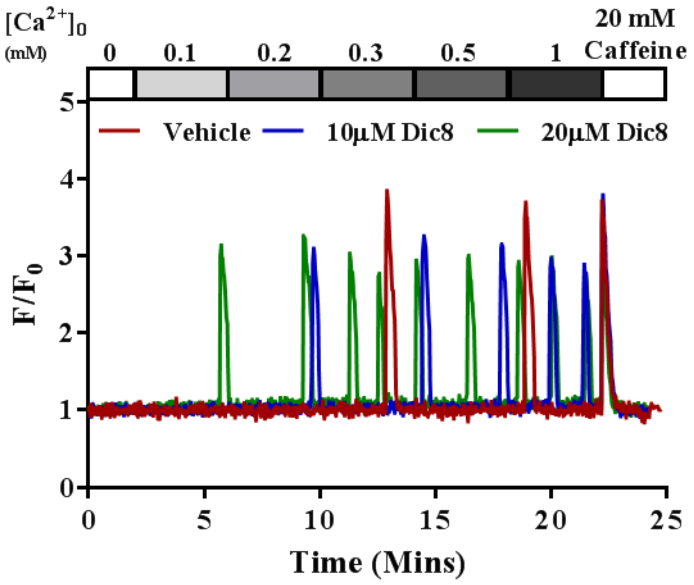

B

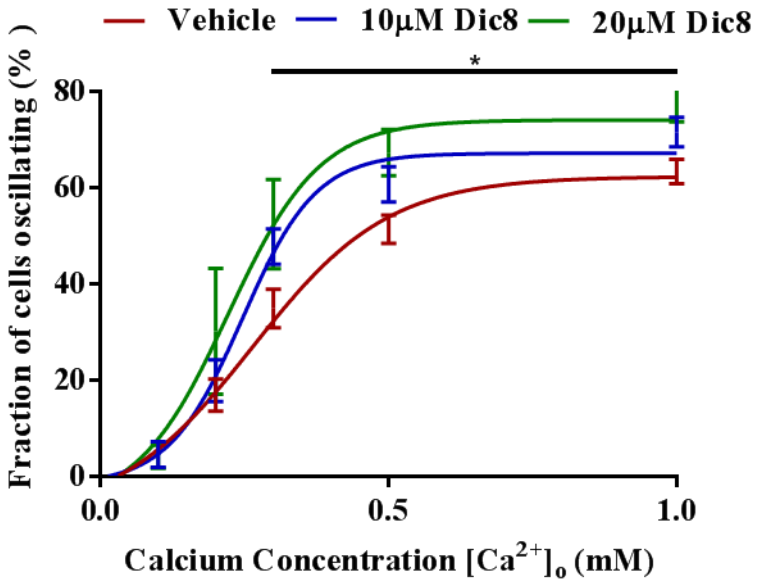

Figure 3.2 Dic8 Increases the Occurrence of SOICR.
HEK293 cells loaded with the cytosolic Ca^{2+} indicator, Fluo-4 AM were superfused with increasing Ca^{2+} concentrations [0, 0.1, 0.2, 0.3, 0.5, 1mM]. (A) Representative Fluo-4 AM trace of cytosolic Ca^{2+} fluorescence, expressed as F/F_0. Bar represents superfusate with length of bar proportional to duration of superfusion. (B) Cumulative fraction of cells exhibiting SOICR at each Ca^{2+} concentration. Vehicle treated HEK293 cells (red line) n = 11, 10µM Dic8 treated HEK293 cells (blue line) n = 8 and 20µM Dic8 treated HEK293 cells (green line) n = 4. n represents number of coverslips per condition, with 150-250 cells counted per coverslip. Data expressed as mean ± SEM.

3.2.1.2 Endogenous PKC Inhibition

A multi-isoform PKC inhibitor, Go6983 was used to determine if inhibition of endogenous PKC influenced SOICR in HEK293 cells. Go6983 inhibits PKC by binding the ATP binding site of the catalytic domain (Sakwe *et al.*, 2005). As described in Section 3.2.1.1, HEK293 cells were loaded with Fluo-4 AM and continuously superfused with KRH containing increasing Ca^{2+} concentrations to elicit SOICR in these cells. SOICR was visualised as transient peaks in the cytosolic Ca^{2+} fluorescence as seen in Figure 3.3 A. The cumulative fraction of cells for each condition (Vehicle treated and 5µM Go6983 treated HEK293 cells) exhibiting Ca^{2+} oscillations was plotted against the concentration of Ca^{2+}. These data points were fitted with a non-linear regression (Vehicle treated HEK293 cells $R^2 = 0.94$ and 5µM Go6983 treated HEK293 cells $R^2 = 0.89$) and statistical significance assessed with a two-way ANOVA with a Sidak's post hoc test. As described in Section 3.2.1.1, an increase in Ca^{2+} concentration results in an increase of fraction of cells undergoing SOICR seen in Figure 3.3 A. Figure 3.3 B shows that inhibition of endogenous PKC in HEK293 cells using Go6983 results in an increase in the percentage of cells undergoing SOICR compared to the mock transfected HEK293 cells at 0.2 (40.2 ± 4.82 versus 16.83 ± 3.07), 0.3 (57.42 ± 4.49 versus 33.03 ± 2.37), 0.5 (66.37 ± 3.25 versus 45.61 ± 1.96) and 1 mM Ca^{2+} (75.11 ± 2.41 versus 53.86 ± 0.69) ($p < 0.0001$ for all points). Whilst performing this assay a member in the lab has shown that the use of ATP inhibitors directly affects the RyR2, resulting in an increase in the occurrence of SOICR, therefore, I discontinued using Go6983 for the rest of the study as any results obtained could be due a direct effect on RyR2 rather than through the modification of PKC activity.

A

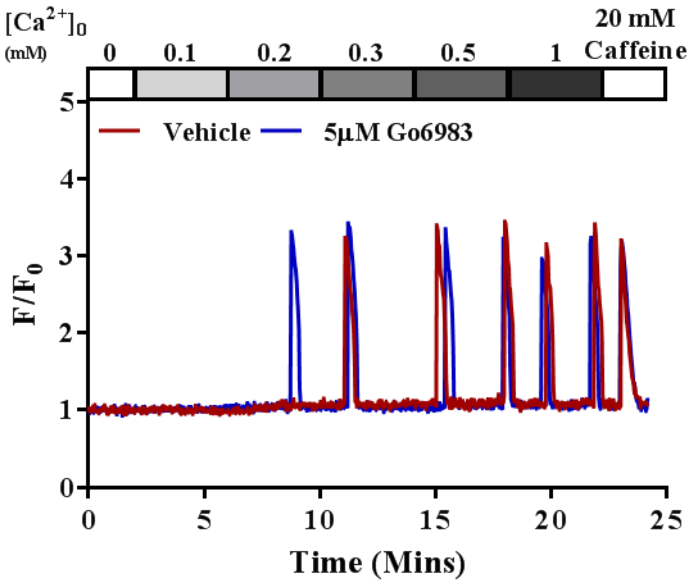

B

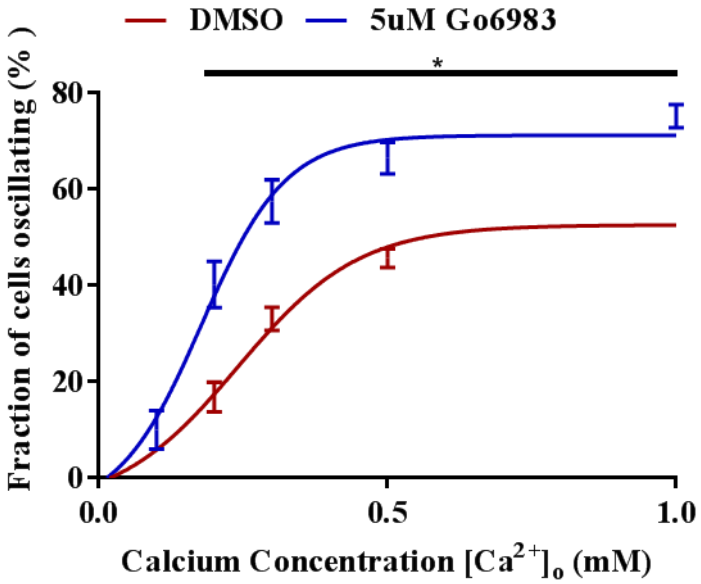

Figure 3.3 Go6983 Increases the Occurrence of SOICR.
HEK293 cells loaded with the cytosolic Ca^{2+} indicator, Fluo-4 AM were superfused with increasing Ca^{2+} concentrations [0, 0.1, 0.2, 0.3, 0.5, 1mM]. (A) Representative Fluo-4 AM trace of cytosolic Ca^{2+} fluorescence, expressed as F/F_0. Bar represents superfusate with length of bar proportional to duration of superfusion. (B) Cumulative fraction of cells exhibiting SOICR at each Ca^{2+} concentration. Vehicle treated HEK293 cells (red line) n = 7 and 5uM Go6983 treated HEK293 cells (blue line) n = 8. n represents number of coverslips per condition, with 150-250 cells counted per coverslip. Data expressed as mean ± SEM.

3.3 PKCα Overexpression

As activation of endogenous PKC led to an increase in SOICR, I next explored which isoform could be responsible.

3.3.1 Western Blot Analysis

Before determining the functional effect of increasing PKCα expression I first determined the endogenous PKCα expression level (the prevalent isoform in HEK293 cells) and increase obtained by transfecting with PKCα, cDNA using western blotting. Cell lysates harvested from HEK293 cells transfected with or without PKCα cDNA were loaded into a 6% (RyR2) and 12% polyacrylamide gels (PKC and GAPDH) to allow protein separation based on their molecular weight using SDS-PAGE. Following wet-transfer of the proteins onto a nitrocellulose membrane, primary and secondary antibodies followed by enhanced chemiluminescence was used to visualise the proteins of interest; RyR2, PKCα, and GAPDH. A protein ladder was used to confirm the molecular weight of the protein of interest. The expression of each protein of interest (RyR2 and PKC) was normalised with GAPDH and modified to represent fold changes. Statistical significance was assessed with an unpaired t-test. The RyR2 protein band appeared above the 250 kDa protein ladder band as RyR2 has an expected weight of 563 kDa. The PKCα and GAPDH protein bands appeared to be adjacent to the protein ladder bands of 75 kDa and 37 kDa aligning with their respective expected weight of 75 kDa and 37 kDa. Figure 3.4 C shows representative images of the total RyR2, PKCα and GAPDH bands at each condition. As seen in Figure 3.4 B, PKCα transfected HEK293 cells resulted in an approximately 5.5-fold increase in total PKCα compared to that of mock transfected HEK293 cells (5.45 ± 0.41 versus 1 ± 0.11) ($p = 0.0005$). PKCα transfected HEK293 cells resulted in no change in total RyR2 compared to that of mock seen in Figure 3.4 C (0.79 ± 0.22 versus 1 ± 0.16) ($p = 0.48$).

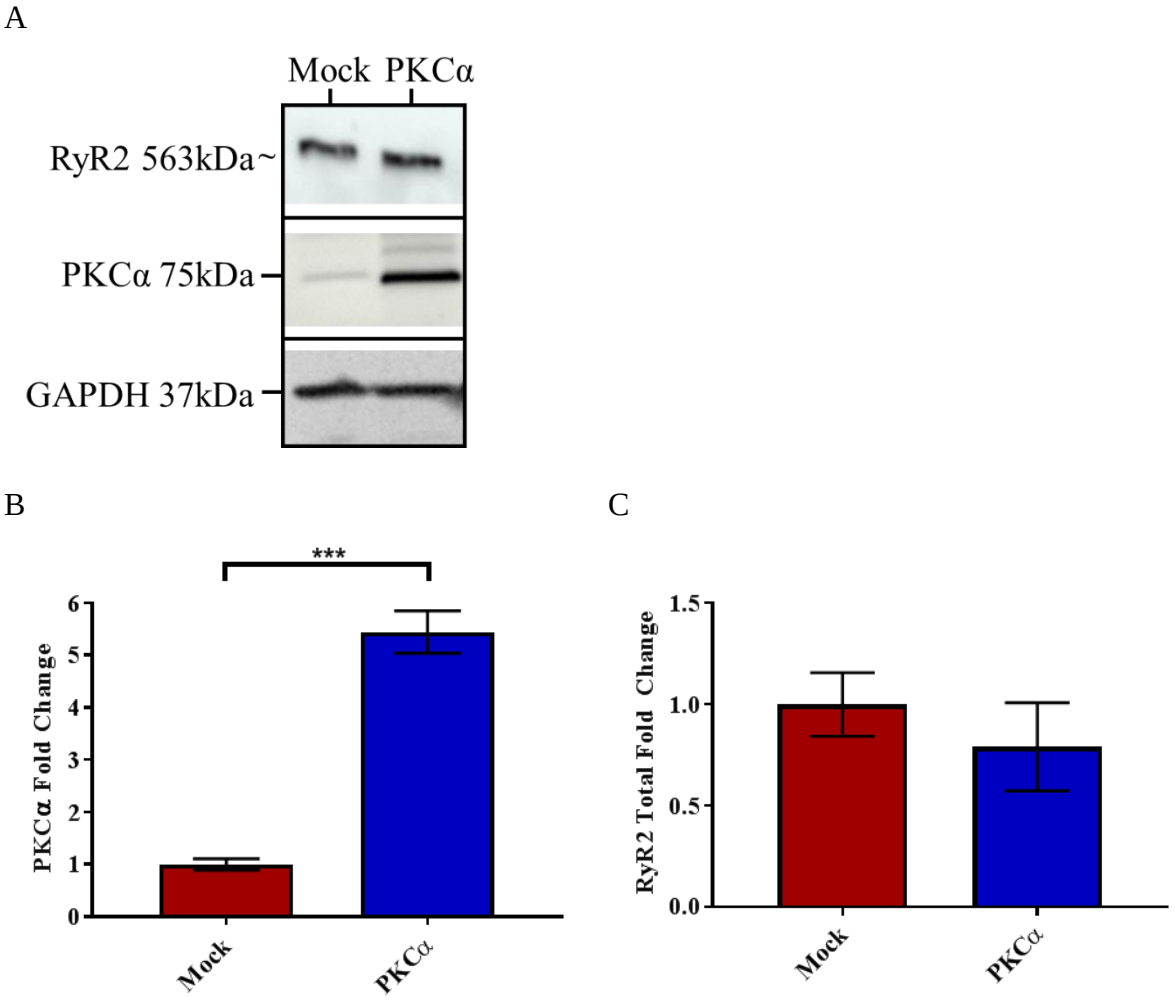

Figure 3.4 PKCα Transfection Results in Robust Expression.
Western blot analysis of harvested HEK293 cell lysates with or without PKCα were developed and analysed. (A) Images of RyR2, PKCα and GAPDH total protein bands for PKCα and mock transfected HEK293 cell lysates. (B) PKCα total normalised against GAPDH and adjusted to show fold changes of protein for PKCα transfected HEK293 cells (blue bar) against the mock transfected HEK293 cells (red bar) n = 3 independent lysates per condition. (C) RyR2 total normalised against GAPDH and adjusted to show fold changes of protein for PKCα transfected HEK293 cells (blue bar) against the mock transfected HEK293 cells (red bar) n = 3 independent lysates per condition. Data expressed as mean ± SEM.

3.3.2 Cytosolic Ca^{2+} Imaging

3.3.2.1 PKCα Overexpression

Not only is PKCα the most expressed PKC isoform in the heart, but PKCα has been shown to have an increase expression/activity in DM. As seen in Figure 3.2 B, activation of endogenous PKC increased the incidence of SOICR; however, the isoform(s) responsible are unknown.

As PKCα is the isoform with the highest expression in the heart, HEK293 cells were transfected with or without PKCα and its effect on SOICR was assessed. As described in Section 3.2.1.1, HEK293 cells were loaded with Fluo-4 AM and continuously superfused with KRH containing increasing Ca^{2+} concentrations to elicit SOICR. SOICR was visualised as transient peaks in the cytosolic Ca^{2+} fluorescence (Figure 3.5 A). The cumulative fraction of cells for each condition (Mock transfected and PKCα transfected HEK293 cells) exhibiting Ca^{2+} oscillations was plotted against the concentration of Ca^{2+}. These data points were fitted with a non-linear regression (Mock transfected HEK293 cells $R^2 = 0.83$ and PKCα transfected HEK293 cells $R^2 = 0.84$) and statistical significance assessed with a two-way ANOVA with a Sidak's post hoc test. As mentioned in Section 3.2.1.1, an increase in Ca^{2+} concentration results in an increase of fraction of cells undergoing SOICR seen in Figure 3.5 A. PKCα transfected HEK293 cells had an increase in the percentage of cells undergoing SOICR compared to the mock transfected HEK293 cells at 0.3 mM Ca^{2+} (34.04 ± 2.69 versus 24.91 ± 3.84) ($p = 0.047$). PKCα transfected HEK293 cells appeared to have no changes in the percentage of cells undergoing SOICR at 0.1, 0.2, 0.5 and 1mM Ca^{2+}.

A

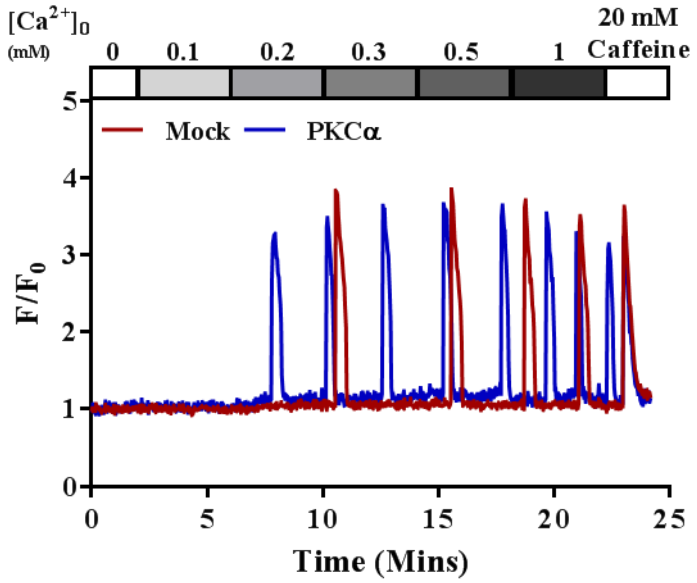

B

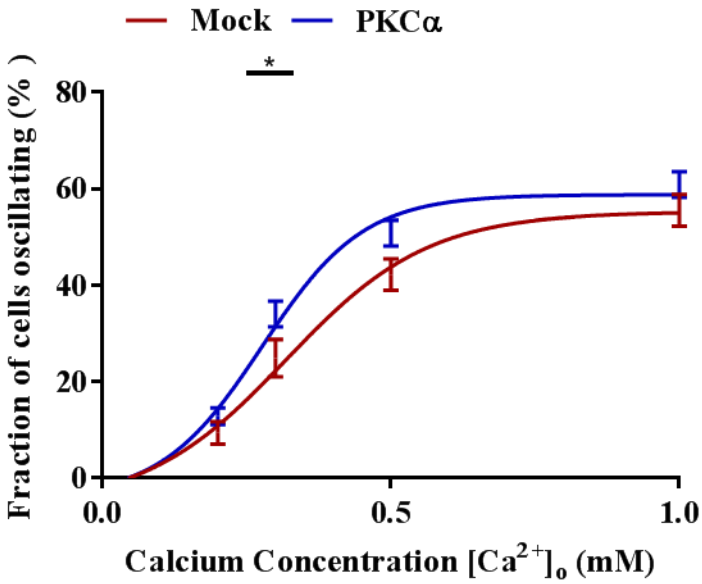

Figure 3.5 PKCα has a Small Effect on the Occurrence of SOICR.
HEK293 cells loaded with the cytosolic Ca^{2+} indicator, Fluo-4 AM were superfused with increasing Ca^{2+} concentrations [0, 0.1, 0.2, 0.3, 0.5, 1mM]. (A) Representative Fluo-4 AM trace of cytosolic Ca^{2+} fluorescence, expressed as F/F_0. Bar represents superfusate with length of bar proportional to duration of superfusion. (B) Cumulative fraction of cells exhibiting SOICR at each Ca^{2+} concentration. Mock transfected HEK293 cells (red line) n = 13 and PKC transfected HEK293 cells (blue line) n = 25. n represents number of coverslips per condition, with 150-250 cells counted per coverslip. Data expressed as mean ± SEM.

3.3.2.2 PKCα Overexpression and Activation with Dic8

Figure 3.5 B shows overexpression of PKCα results in a small change in the incidence of SOICR. Based on Figure 3.2 B, showing that activation of endogenous PKC with Dic8 increased the incidence of SOICR I decided to see if PKCα overexpression with or without Dic8 could further increase the incidence of SOICR. As described in Section 3.2.1.1, HEK293 cells were loaded with Fluo-4 AM and continuously superfused with KRH containing increasing Ca^{2+} concentrations to elicit SOICR in these cells. SOICR was visualised as transient peaks in the cytosolic Ca^{2+} fluorescence as seen in Figure 3.6 A. The cumulative fraction of cells for each condition (Vehicle treated and 10µM Dic8 treated PKCα transfected HEK293 cells) exhibiting Ca^{2+} oscillations was plotted against the concentration of Ca^{2+}. These data points were fitted with a non-linear regression (Vehicle treated PKCα transfected HEK293 cells $R^2 = 0.82$ and 10µM Dic8 treated PKCα transfected HEK293 cells $R^2 = 0.84$) and statistical significance assessed with a two-way ANOVA with a Sidak's post hoc test. Consistent with Section 3.2.1.1, an increase in Ca^{2+} concentration resulted in an increase of fraction of cells undergoing SOICR seen in Figure 3.6 A. I initially believed that PKCα overexpression may have only shown a small effect on SOICR, seen in Figure 3.5 due to a lack of agonists, however, in Figure 3.6 B, there was no change in the percentage of cells undergoing SOICR between the PKCα transfected HEK293 cells treated with or without the PKC agonist, Dic8, at all Ca^{2+} concentrations ($p > 0.05$) suggesting that PKCα may not be responsible for the increase in SOICR observed due to Dic8 treatment alone (Figure 3.5).

A

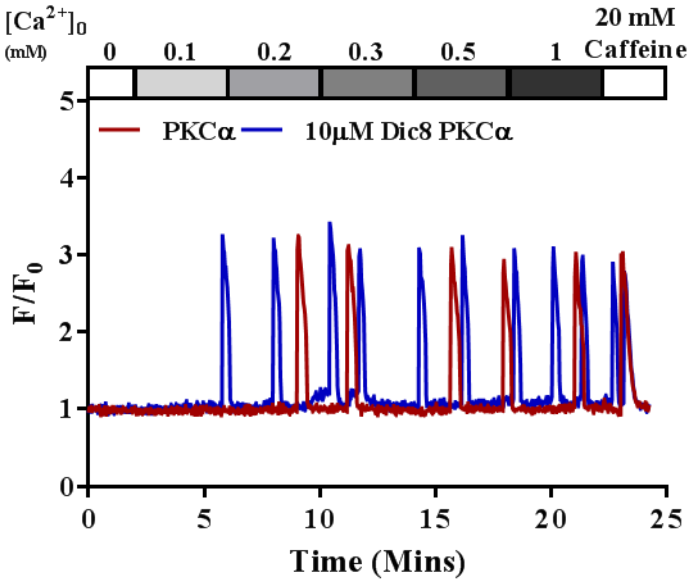

B

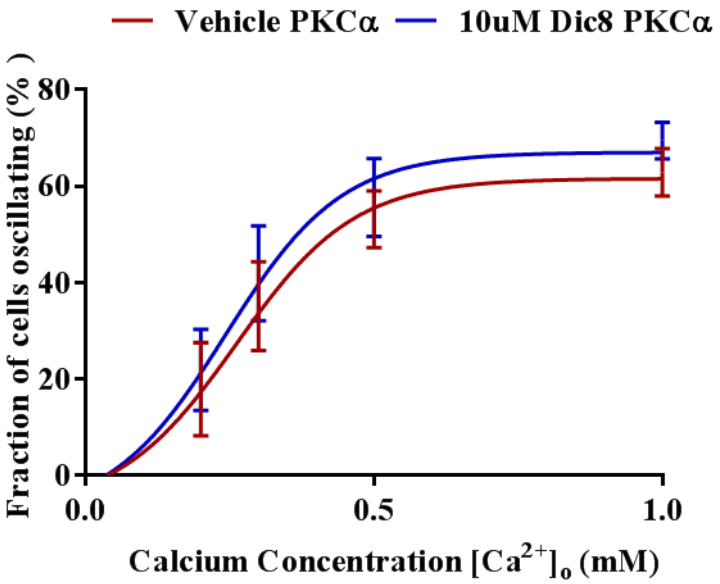

Figure 3.6 Dic8 does not Further Increase the Effect of PKCα Overexpression.
HEK293 cells loaded with the cytosolic Ca^{2+} indicator, Fluo-4 AM were superfused with increasing Ca^{2+} concentrations [0, 0.1, 0.2, 0.3, 0.5, 1mM]. (A) Representative Fluo-4 AM trace of cytosolic Ca^{2+} fluorescence, expressed as F/F_0. Bar represents superfusate with length of bar proportional to duration of superfusion. (B) Cumulative fraction of cells exhibiting SOICR at each Ca^{2+} concentration. Vehicle treated PKCα transfected HEK293 cells (red line) n = 4 and Dic8 treated PKCα transfected HEK293 cells (blue line) n = 4. n represents number of coverslips per condition, with 150-250 cells counted per coverslip. Data expressed as mean ± SEM.

3.3.3 Luminal Ca^{2+} Imaging

3.3.3.1 PKCα Overexpression

To confirm the small effect of PKCα on the occurrence of SOICR in Figure 3.5, SR store dynamics were assessed. HEK293 cells were transfected with the luminal Ca^{2+} indicator protein, D1ER and continuously superfused with KRH containing increasing Ca^{2+} concentrations (0, 1, 2 mM) to elicit SOICR in these cells. To fill the Ca^{2+} store to maximum, HEK293 cells were superfused with a 2 mM Ca^{2+} KRH solution containing 2 mM tetracaine which blocks RyR2. Finally, to deplete the Ca^{2+} store, HEK293 cells were superfused with 2 mM Ca^{2+} KRH solution containing 20 mM caffeine. F_{max}, F_{min}, F_{SOICR} and F_{termi} parameters were determined from the single cell luminal Ca^{2+} fluorescence traces and normalised to F_{min} to calculate SOICR characteristics, seen in Figure 3.7 A. The percentage of store size ($F_{max} - F_{min}$), release threshold ($[F_{SOICR} - F_{min}] / [F_{max} - F_{min}] \times 100$) and termination threshold ($[F_{termi} - F_{min}] / [F_{max} - F_{min}] \times 100$) were calculated for each condition (Mock transfected HEK293 cells and PKCα transfected HEK293 cells) and statistical significance was assessed with an unpaired two-tailed student's t-test. Figure 3.7 B and Figure 3.7 C shows PKCα results in no change in the total store size and release threshold between mock and PKCα transfected HEK293 cells ($p > 0.05$), inconsistent with the small change in SOICR observed in Figure 3.5 B. Figure 3.7 D shows that PKCα transfected HEK293 cells have an increased termination threshold compared to the mock transfected HEK293 (48 ± 1.96 versus 43.4 ± 1.01) ($p = 0.038$).

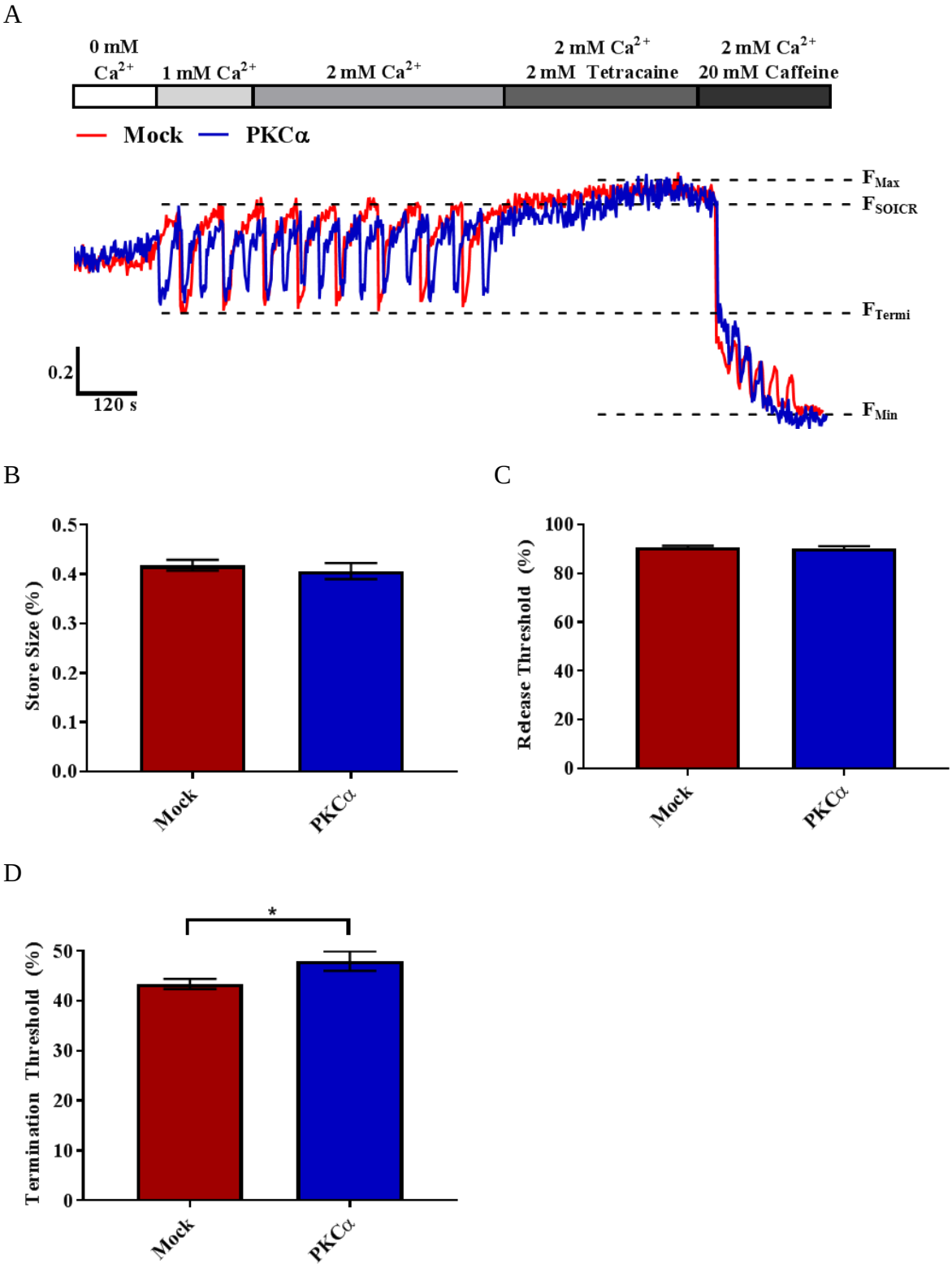

Figure 3.7 PKCα Reduces Store Size.
HEK293 cells transfected with the luminal Ca^{2+} indicator protein, D1ER were superfused with increasing Ca^{2+} concentrations [0,1, 2mM] followed by tetracaine and caffeine. (A) Representative D1ER trace luminal Ca^{2+} fluorescence, expressed as F/F_0. Bar represents superfusate with length of bar proportional to duration of superfusion. Bar graph of the percentage of (B) store size, (C) release threshold and (D) termination threshold for each condition. Mock transfected HEK293 cells (red bar) n = 110 and PKCε transfected HEK293 cells (blue bar) n = 30. n represents the number of cells per condition. Data expressed as mean ± SEM.

3.3.3.2 PKCα Overexpression and Activation with Dic8

To determine the effect of PKCα plus Dic8 on the occurrence of SOICR, seen in Figure 3.6, SR store dynamics were also assessed and compared against the results from Figure 3.7.

HEK293 cells were co-transfected with PKCα and the luminal Ca^{2+} indicator protein, D1ER and continuously superfused with KRH containing increasing Ca^{2+} concentrations (0, 1, 2 mM) to elicit SOICR in these cells. To fill the Ca^{2+} store to maximum, HEK293 cells were superfused with a 2 mM Ca^{2+} KRH solution containing 2 mM tetracaine which blocks RyR2. Finally, to deplete the Ca^{2+} store, HEK293 cells were superfused with 2 mM Ca^{2+} KRH solution containing 20 mM caffeine. F_{max}, F_{min}, F_{SOICR} and F_{termi} parameters were determined from the single cell luminal Ca^{2+} fluorescence traces and normalised to F_{min} to calculate SOICR characteristics. The percentage of store size ($F_{max} - F_{min}$), release threshold ($[F_{SOICR} - F_{min}] / [F_{max} - F_{min}] \times 100$) and termination threshold ($[F_{termi} - F_{min}] / [F_{max} - F_{min}] \times 100$) were calculated for Dic8 treated PKCα transfected HEK293 cells, and statistical significance was assessed with a one-way ANOVA. Figure 3.8 A and C shows no change in the total store size and termination threshold between the mock, PKCα transfected, and PKCα transfection with Dic8 ($p > 0.05$). Figure 3.8 B shows that PKCα transfection with Dic8 results in a significant decrease in the release threshold compared to the mock and PKCα transfected HEK293 cells (85.56 ± 1.51 versus 90.77 ± 0.53 and 90.39 ± 0.74) (p = 0.001, 0.006). The reduction in the release threshold of SOICR could either be due to PKCα being further activated with Dic8 or an independent effect of Dic8. An independent effect of Dic8 on the release threshold for SOICR would be consistent with the increase in the occurrence of SOICR observed in Figure 3.2.

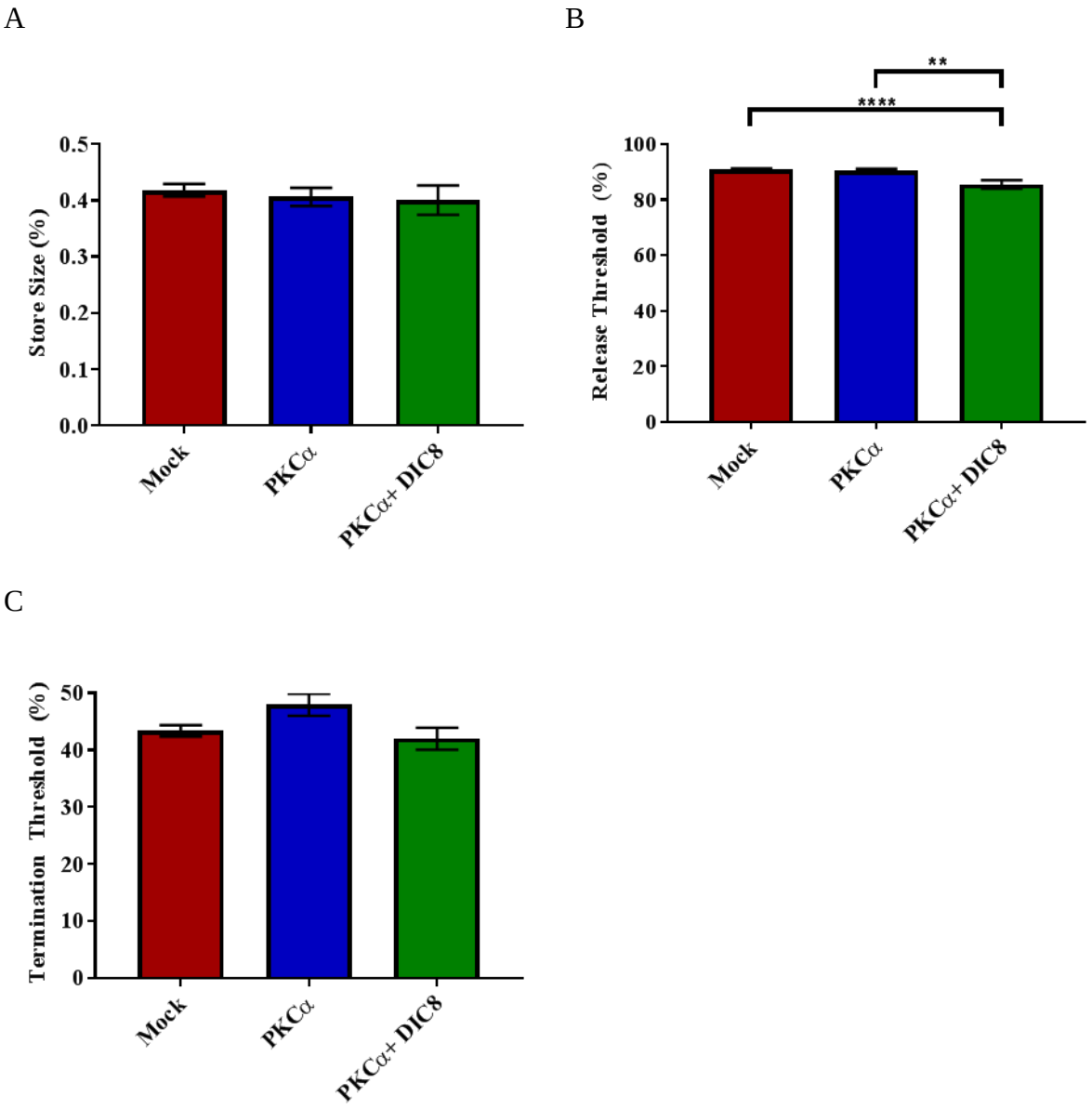

Figure 3.8 Overexpression of PKCα with Dic8 Reduces Release Threshold.
HEK293 cells transfected with the luminal Ca^{2+} indicator protein, D1ER were superfused with increasing Ca^{2+} concentrations [0,1, 2mM] followed by tetracaine and caffeine. Bar graph of the percentage of (A) store size, (B) release threshold and (C) termination threshold for each condition. Mock transfected HEK293 cells (red bar) n = 110, PKCε transfected HEK293 cells (blue bar) n = 30 and Dic8 treated PKCε transfected HEK293 cells (green bar) n = 27. n represents the number of cells per condition. Data expressed as mean ± SEM.

3.4 PKCε Overexpression

3.4.1 Cytosolic Ca^{2+} Imaging

3.4.1.1 PKCε Overexpression

As endogenous activation of PKC in HEK293 cells using Dic8 resulted in an increase in the occurrence of SOICR (Figure 3.2 B) and PKCα isoform appears to have only a small effect on the occurrence of SOICR (Figure 3.5 B), the next logical step was to determine the effect of other PKC isoforms, specifically PKCε, which is also expressed in HEK293 cells. PKCε differs from PKCα based on the structure and its mode of activation, as it requires only DAG and not Ca^{2+}. PKCε is also highly expressed in the heart and has also been shown to have an increased expression/activity in DM. As described in Section 3.2.1.1, HEK293 cells were loaded with Fluo-4 AM and continuously superfused with KRH containing increasing Ca^{2+} concentrations to elicit SOICR in these cells. SOICR was visualised as transient peaks in the cytosolic Ca^{2+} fluorescence as seen in Figure 3.9 A. The cumulative fraction of cells for each condition (Mock transfected and PKCε transfected HEK293 cells) exhibiting Ca^{2+} oscillations was plotted against the concentration of Ca^{2+}. These data points were fitted with a non-linear regression (Mock transfected HEK293 cells $R^2 = 0.88$ and PKCε transfected HEK293 cells $R^2 = 0.86$) and statistical significance assessed with a two-way ANOVA with a Sidak's post hoc test. As in Section 3.2.1.1, an increase in Ca^{2+} concentration results in an increase of fraction of cells undergoing SOICR seen in Figure 3.9 A. PKCε transfected HEK293 cells had an increase in the percentage of cells undergoing SOICR compared to the mock transfected HEK293 cells at 0.5 (62.61 ± 5.1 versus 40.33 ± 3.06) ($p = 0.0008$) and 1 mM Ca^{2+} (70.8 ± 4.43 versus 45.6 ± 2.67) ($p = 0.0001$).

A

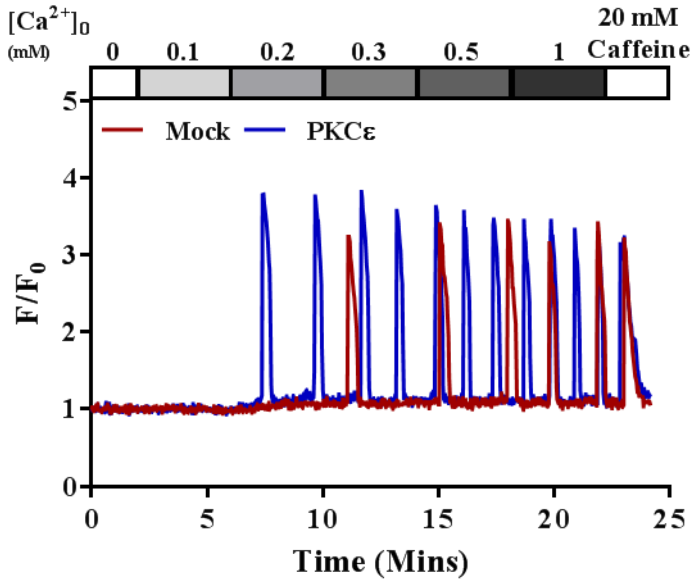

B

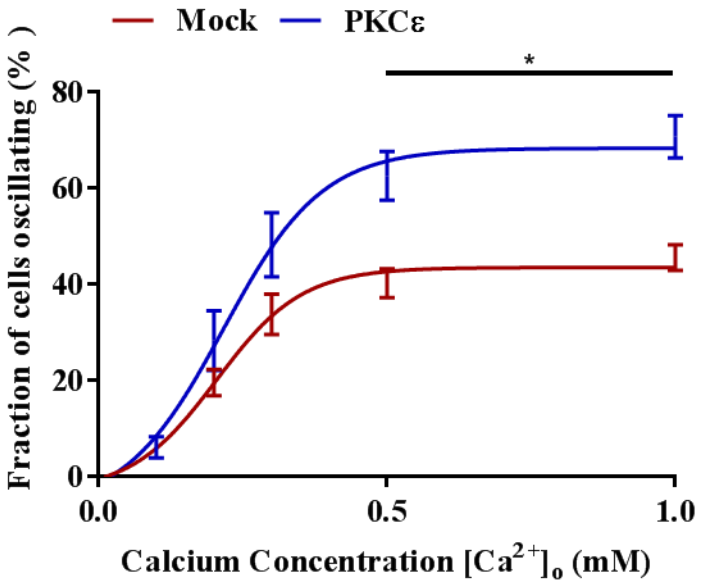

Figure 3.9 PKCε Increases the Occurrence of SOICR.
HEK293 cells loaded with the cytosolic Ca^{2+} indicator, Fluo-4 AM were superfused with increasing Ca^{2+} concentrations [0, 0.1, 0.2, 0.3, 0.5, 1mM]. (A) Representative Fluo-4 AM trace of cytosolic Ca^{2+} fluorescence, expressed as F/F_0. Bar represents superfusate with length of bar proportional to duration of superfusion. (B) Cumulative fraction of cells exhibiting SOICR at each Ca^{2+} concentration. Mock transfected HEK293 cells (red line) n = 6 and PKCε transfected HEK293 cells (blue line) n = 6. n represents number of coverslips per condition, with 150-250 cells counted per coverslip. Data expressed as mean ± SEM.

3.4.1.2 PKCε Overexpression and Activation with Dic8

Figure 3.9 B showed transfection of PKCε results in a significant increase in the incidence of SOICR in HEK293 cells. Based on Figure 3.2 B, showing that activation of endogenous PKC with Dic8 increased the incidence of SOICR I decided to see if PKCε overexpression with or without Dic8 could increase the incidence of SOICR even further. As described in Section 3.2.1.1, HEK293 cells were loaded with Fluo-4 AM and continuously superfused with KRH containing increasing Ca^{2+} concentrations to elicit SOICR in these cells. SOICR was visualised as transient peaks in the cytosolic Ca^{2+} fluorescence as seen in Figure 3.10 A. The cumulative fraction of cells for each condition (Vehicle treated and 10μM Dic8 treated PKCε transfected HEK293 cells) exhibiting Ca^{2+} oscillations was plotted against the concentration of Ca^{2+}. These data points were fitted with a non-linear regression (Vehicle treated PKCε transfected HEK293 cells $R^2 = 0.95$ and 10μM Dic8 treated PKCε transfected HEK293 cells $R^2 = 0.93$) and statistical significance assessed with a two-way ANOVA with a Sidak's post hoc test. As in Section 3.2.1.1, an increase in Ca^{2+} concentration results in an increase of fraction of cells undergoing SOICR seen in Figure 3.10 A. In Figure 3.10 B, there was no change in the percentage of cells undergoing SOICR between the PKCε transfected HEK293 cells treated with or without Dic8 at all Ca^{2+} concentrations ($p > 0.05$), suggesting the overexpressed PKCε activity cannot be further increased using the PKC agonist, Dic8.

A

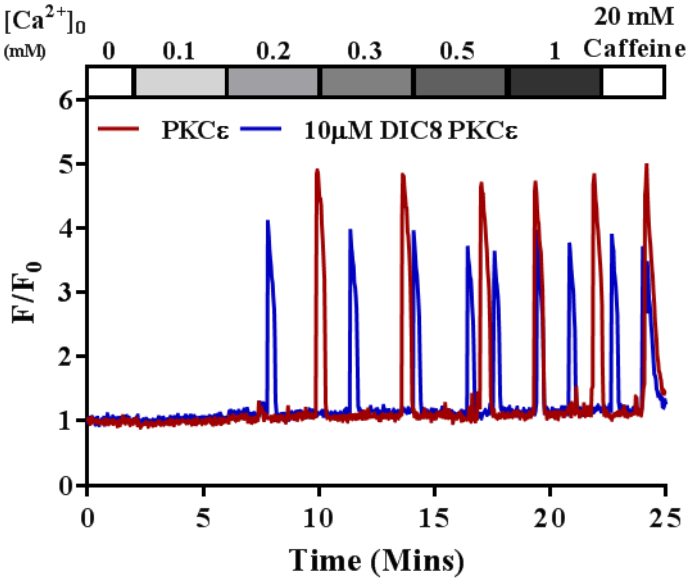

B

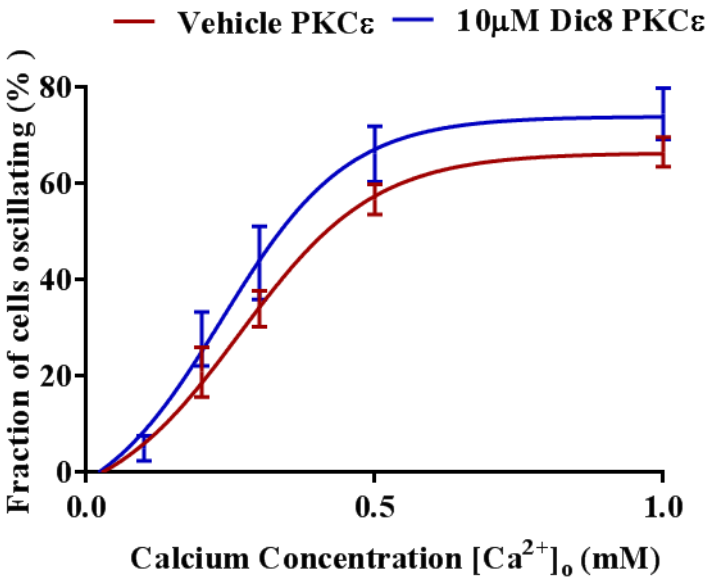

Figure 3.10 Dic8 does not Further Increase the Effect on the Occurrence of SOICR in Cells Transfected with PKCε.

HEK293 cells loaded with the cytosolic Ca^{2+} indicator, Fluo-4 AM were superfused with increasing Ca^{2+} concentrations [0, 0.1, 0.2, 0.3, 0.5, 1mM]. (A) Representative Fluo-4 AM trace of cytosolic Ca^{2+} fluorescence, expressed as F/F_0. Bar represents superfusate with length of bar proportional to duration of superfusion. (B) Cumulative fraction of cells exhibiting SOICR at each Ca^{2+} concentration. Vehicle treated PKCε transfected HEK293 cells (red line) n = 4 and Dic8 treated PKCε transfected HEK293 cells (blue line) n = 4. n represents number of coverslips per condition, with 150-250 cells counted per coverslip. Data expressed as mean ± SEM.

3.4.2 Luminal Ca^{2+} Imaging

3.4.2.1 PKCε Overexpression

To confirm the effect of PKCε on the occurrence of SOICR in Figure 3.9, SR store dynamics were also assessed. HEK293 cells were co-transfected with PKCε and the luminal Ca^{2+} indicator protein, D1ER. As described in Section 2.3.3.1, cells are continuously superfused with different KRH solutions; 0, 1, 2 mM Ca^{2+}, 2 mM Ca^{2+} with 2 mM tetracaine and 2 mM Ca^{2+} with 20 mM caffeine. F_{max}, F_{min}, F_{SOICR} and F_{termi} parameters were determined from the single cell luminal Ca^{2+} fluorescence traces and normalised to F_{min} to calculate SOICR characteristics, seen in Figure 3.11 A. The percentage of store size ($F_{max} - F_{min}$), release threshold ($[F_{SOICR} - F_{min}] / [F_{max} - F_{min}] \times 100$) and termination threshold ($[F_{termi} - F_{min}] / [F_{max} - F_{min}] \times 100$) were calculated for each condition (Mock transfected HEK293 cells and PKCε transfected HEK293 cells) and statistical significance was assessed with an unpaired two-tailed student's t-test. Figure 3.11 B shows no change in the total store size between the PKCε and mock transfected HEK293 cells ($p = 0.85$). Figure 3.11 C and Figure 3.11 D show that PKCε transfected HEK293 cells resulted in a decrease in both termination threshold (38.22 ± 1.61 versus 43.4 ± 1.01) ($p = 0.005$) and release threshold (87.47 ± 1.07 versus 90.77 ± 0.53) ($p = 0.002$) respectively, consistent with the increase in SOICR observed in Figure 3.9 B.

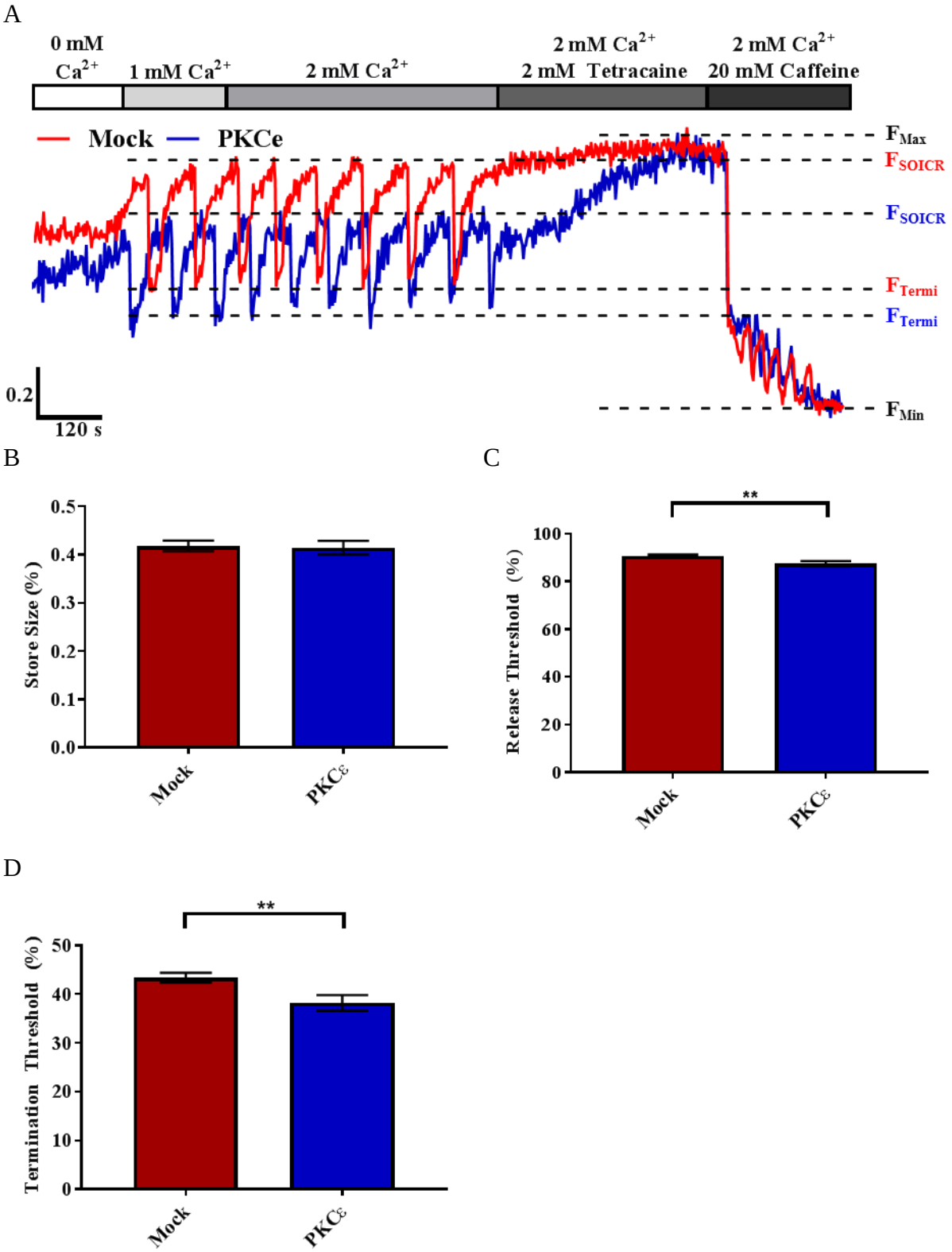

Figure 3.11 PKCε reduces release and termination threshold.
HEK293 cells transfected with the luminal Ca^{2+} indicator protein, D1ER were superfused with increasing Ca^{2+} concentrations [0,1, 2mM] followed by tetracaine and caffeine. (A) Representative D1ER trace luminal Ca^{2+} fluorescence. Bar represents superfusate with length of bar proportional to duration of superfusion. Bar graph of the percentage of (B) store size, (C) release threshold and (D) termination threshold for each condition. Mock transfected HEK293 cells (red bar) n = 110 and PKCε transfected HEK293 cells (blue bar) n = 52. n represents the number of cells per condition. Data expressed as mean ± SEM.

4 Discussion

4.1 Results

In this study, I hypothesised that one of the possible molecular pathways in which DM patients have an increased risk and association with arrhythmia was due to excessive PKC activity, due to an accumulation of DAG, resulting in phosphorylation of RyR2 triggering SOICR a precursor for arrhythmogenesis. To test this hypothesis, I first looked at the effect of activation or inhibition of endogenous PKC in HEK293 cells on the occurrence of SOICR. My results showed that activation of PKC using Dic8 increased the occurrence of SOICR, suggesting that one or many of the PKC isoforms expressed endogenously in HEK293 can phosphorylate the RyR2, resulting in the increase in SOICR (Figure 3.2). I then showed that when inhibiting endogenous PKC in HEK293 cells, using Go6983, there is a massive increase in the occurrence of SOICR; this was unexpected as an increased activity of endogenous PKC also showed an increase in the occurrence of SOICR (Figure 3.3). The result of increased and decreased endogenous PKC activity in HEK293 suggests that that either Dic8 or Go6983 may have effects on proteins other than PKC or that modulation of PKC in HEK293 cells alters multiple pathways linked to SOICR. Through the work of others in the lab, we found that Go6983 is likely to be affecting RyR2 directly (See Section 4.1.2). Disregarding the effect of Go6983 my other data suggest that activation of PKC increases the incidence of SOICR as hypothesised.

As it was unclear which PKC isoform/s resulted in an increase of SOICR occurrence using Dic8, I next aimed to determine the isoform responsible. I chose to start with examining the effect of PKCα on the occurrence of SOICR, as it has the highest isoform expression in the human heart (Simonis *et al.*, 2007). To look at the effect of PKCα I overexpressed this isoform in my HEK293 cell model. Western blot analysis showed that PKCα was successfully transfected, where its expression increased by 5.5-fold when transfected with PKCα cDNA

(Figure 3.4). My research showed that overexpression of PKCα in HEK293 cells resulted in a small increase in the occurrence of SOICR at low Ca^{2+} concentrations, which suggests that PKCα is unlikely to be the isoform responsible for the effect of endogenous activation of PKC in HEK293 cells (Figure 3.5). As a cPKC isoform, PKCα requires both Ca^{2+} and DAG for activation, hence when I overexpressed PKCα in HEK293 cells, I was uncertain if there are enough substrates (DAG or Ca^{2+}) for activation. As activation of endogenous PKC using Dic8 increased SOICR occurrence, I looked at the effect of overexpressed PKCα, with or without Dic8. My results showed that PKCα plus Dic8 did not result in an increase in SOICR occurrence compared to PKCα alone, suggesting that PKCα may not be phosphorylating the RyR2, resulting in SOICR (Figure 3.6) under the conditions used in my assay. To further investigate whether PKCα affects SR dynamics, HEK293 cells were co-transfected with both D1ER and PKCα. My results show that overexpression of PKCα does not alter the SR store size or the release threshold for SOICR, but instead results in an increase in the termination threshold, suggesting overexpressed PKCα in HEK293 cells has no effect on increasing the occurrence of SOICR but may actually reduce the magnitude of release (Figure 3.7). To then investigate the whether PKCα with Dic8 affects SR dynamics, HEK293 cells were co-transfected with both D1ER and PKCα, then treated with or without Dic8. My results show that overexpression of PKCα with Dic8 show a decrease in the release threshold, suggesting overexpression of PKCα with Dic8 should result in an increase in the occurrence of SOICR (Figure 3.8). Interestingly to note is that the significant increase in the termination threshold by overexpressed PKCα in Figure 3.7 is lost when using a one-way ANOVA with three conditions.

Following on from PKCα, I then decided to test a nPKC isoform that also has high expression in the heart, PKCε, to see if there is a difference between the cPKC and nPKC subclasses. The rationale for looking at a nPKC was that they do not need Ca^{2+} to be activated, just DAG which I could add exogenously if required. My research showed that overexpression of PKCε in

HEK293 cells resulted in a dramatic increase in the occurrence of SOICR (Figure 3.9). This suggests that PKCε may be one of the isoforms responsible for the increase in SOICR occurrence due to endogenous activation of PKC in HEK293 cells, as these cells express PKCε endogenously (Sakwe *et al.*, 2004). As PKCε only requires DAG for activation, the addition of Dic8 in HEK293 cells with overexpressed PKCε may result in a greater level of activity. When I looked at the effect of overexpressed PKCε, with or without Dic8, my results showed that PKCε with Dic8 did not result in a further increase in SOICR occurrence, suggesting that the overexpressed PKCε was already fully activated by endogenous DAG (Figure 3.10). As HEK293 cell were grown in high glucose concentrations their DAG levels could already be very high (Ayo *et al.*, 1991). To understand the mechanism behind the increased occurrence of SOICR seen in overexpression of PKCε, I looked at its effect on SR dynamics. HEK293 cells were co-transfected with D1ER and PKCε, and my results show that overexpression of PKCε does not alter the SR store size and instead results in a decrease in both the release and termination thresholds for SOICR (Figure 3.11). This suggests that PKCε phosphorylates the RyR2 decreasing the release threshold for SOICR making it more likely to be surpassed increasing the incidence of SOICR. This is consistent with the proposed effects of PKA and CaMKII phosphorylation of RyR2 (Xiao *et al.*, 2007; McCauley & Wehrens, 2011).

4.1.1 PKC Activation Effect on SOICR

As hypothesised, Dic8 increased the occurrence of SOICR in endogenous HEK293 cells. As Dic8 is a DAG analogue, the effect in seen HEK293 cells would most likely be due to the activation of cPKC and/or nPKC, but not an aPKC, as aPKCs require phosphatidylinositols for activation (Xiao & Liu, 2013).

4.1.2 PKC Inhibition Effect on SOICR

Go6983 increased the occurrence of SOICR in HEK293 cells. This was inconsistent with the effect of activation of PKC and contradictory to what I had hypothesised. However, Go6983 inhibits PKC by binding to the ATP site within the catalytic domain of PKC, preventing PKC function. Currently, a Ph.D. project in the lab is looking at the effect of ATP-based kinase inhibitors and their effect on RyR2 and SOICR. The results thus far show that many ATP-based kinase inhibitors directly activate the RyR2, resulting in SOICR. This suggests that Go6983 may act on RyR2 in a similar way, making any results obtained using this drug difficult to interpret. For this reason, I decided to discontinue the use of Go6983 for the rest of the study. In the future, to determine the effect of inhibiting endogenous PKC in HEK293 cells, I could use Calphostin C; a potent and selective PKC inhibitor that specifically targets the regulatory domain of PKC (Kobayashi *et al.*, 1989). I would expect to see the opposite effect of PKC activation, therefore, a decrease in the occurrence of SOICR along with an increase in the release threshold for SOICR.

4.1.3 Effect of PKCα Overexpression on SOICR

Overexpression of PKCα resulted in no change in the release threshold for SOICR, which was inconsistent with a small increase in the occurrence of SOICR. I, therefore, reject my hypothesis that PKCα would decrease the release threshold for SOICR and increase the SOICR occurrence, as an increase in SOICR occurrence is expected to be matched with a decreased release threshold for SOICR. However, the very small increase in SOICR occurrence would only require a small reduction in the release threshold for SOICR which could have been below the sensitivity of my SR Ca^{2+} measurement assay. Interestingly, PKCα overexpression results in an increase in the termination threshold for SOICR. An increase in termination threshold without a change in release threshold for SOICR would imply a reduction in the fraction of Ca^{2+} release, however, this possibly would have no effect on the occurrence of SOICR. Though, when the

conditions mock, PKCα and PKCα with Dic8 were assessed (Figure 3.8 C), there were no differences seen in the termination threshold, therefore, PKCα possibly has no consistent effect on termination threshold.

Although Figure 3.4 shows that transfection of PKCα increased the total protein level, it gives no indication of misfolded or inactive proteins, therefore, the use of a PKC activity assay could be used to determine the activity of PKCα transfection (Murillo-Carretero *et al.*, 2017).

My results showed that PKCα with Dic8 decreased release threshold for SOICR (Figure 3.8 B). This result could suggest that Dic8 activates the overexpressed PKCα, allowing for a significant reduction in release threshold which would be consistent with the small increase in SOICR occurrence with PKCα. Alternatively, it could be that Dic8 results in a decreased release threshold for SOICR, regardless of the overexpression of PKCα, which is consistent with the increase in the SOICR occurrence seen with Dic8 alone. To confirm if the results shown in Figure 3.8 B is Dic8 independent, luminal Ca^{2+} imaging comparing Dic8 versus vehicle treated HEK293 cells would be performed in the future, where the decrease in the release threshold would be compared to the decrease release threshold in the Dic8 with PKCα overexpression.

4.1.4 Effect of PKCε Overexpression on SOICR

Overexpression of PKCε resulted in a reduction in the termination threshold and release threshold for SOICR which was consistent with the large increase in the occurrence of SOICR. A reduction of the termination threshold means that there is an increase in the amount of Ca^{2+} released during Ca^{2+} release events (CICR and SOICR), whereas a reduction of the release threshold for SOICR means that less Ca^{2+} within the SR is required to activate RyR2, resulting in a SOCIR event. Therefore, I accepted my hypothesis that PKCε can modulate SOICR (the RyR2), as the increase in SOICR occurrence was matched with a decreased release threshold

for SOICR. As mentioned in Section 1.3.1, a reduction of the release threshold can lead to a SOICR event, therefore, severely increasing the occurrence of arrhythmia (Liu *et al.*, 2017). Though the reduction of release threshold for SOICR between PKCε transfection versus mock transfected HEK293 cells seems like a small change (~3% decrease), it is consistent with other studies that looked at RyR2 mutations, that can cause sudden cardiac death, which showed a ~9% reduction in the release threshold for SOICR (Liu *et al.*, 2013).

4.2 Proposed Model of Action of PKCε on SOICR

PKCε results in a reduction of the release threshold and termination threshold, along with an increased occurrence of SOICR, however, the molecular interaction that results in these changes are unknown. The current literature has led us to the deduction that there are three proposed models in which these effects could occur.

4.2.1 PKCε Phosphorylation of RyR2

Kinases that become overexpressed, such as CaMKII and PKA, can lead to RyR2 phosphorylation, resulting in the reduction of the release threshold and termination threshold, increasing the occurrence of SOICR and the amount of Ca^{2+} released (Wehrens *et al.*, 2006). Transgenic mice that had an acute overexpression of CaMKIIδ resulted in an increase in Ca^{2+} leak (SOICR) as well as an increase in RyR2 phosphorylation at S2809 and S2815 (Kohlhaas *et al.*, 2006). I therefore hypothesise that in DM, an increased activity PKCε results in a similar fashion to these kinases through the phosphorylation of the RyR2 resulting in a structural conformational change, resulting in both the reduction of the release threshold for SOICR, thereby increasing Ca^{2+} leak (SOICR) and a reduction in termination threshold, increasing the amount of Ca^{2+} released. As discussed in Section 1.3.1, if the SR Ca^{2+} load exceeds this release threshold for SOICR, it results in RyR2-mediated Ca^{2+} release from the SR, where a reduction

of the release threshold results in a greater risk of SOICR. When SOICR occurs, the increase in cytosolic Ca^{2+} must then be removed, which can result in arrhythmia as described in Section 1.3.1.

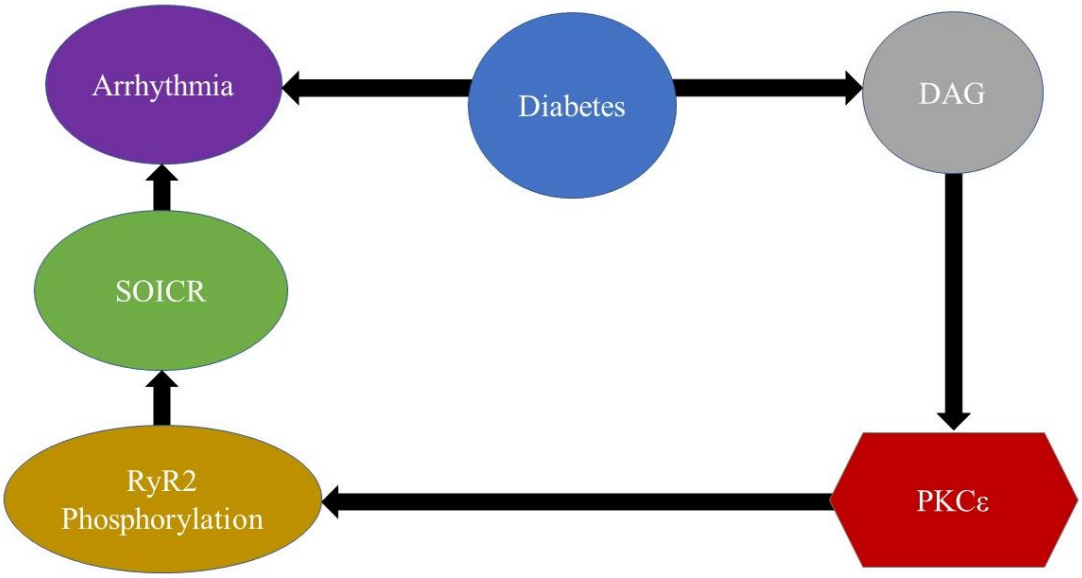

Figure 4.1 Proposed Model: PKCε Mediated Phosphorylation of RyR2 Linking DM to Arrhythmia.
DM has an increase accumulation of DAG which over activates PKCε. PKCε phosphorylates RyR2 resulting in SOICR which leads to arrhythmia.

4.2.2 CaMKII Phosphorylation of RyR2

Another possibility for the increasing occurrence of SOICR along with the decrease in release threshold for SOICR, due to a direct phosphorylation of RyR2 by PKC, could be due to indirect phosphorylation of RyR2. PKCε has been shown to be able to activate NADPH Oxidase Type 2 (NOX2) resulting in reactive oxygen species (ROS) release from the mitochondria, which has been described to be able to cause oxidation-activation of CaMKII, resulting in CaMKII mediated-phosphorylation the RyR2 resulting in SOICR (Erickson *et al.*, 2008; Ho *et al.*, 2014). If in fact the increased synthesis and accumulation of DAG in DM does result in an increase in PKCε leading to increased oxidation, this study may support the proposed model that CaMKII is the major kinase involved in DM arrhythmogenesis (Erickson *et al.*, 2013). Under basal conditions, the CaMKII regulatory domain auto-inhibits the catalytic domain, however, it is well established that oxidised CaMKII results in the dissociation of the regulatory domain from

the catalytic domain, leading to over-activity of the kinase (Erickson *et al.*, 2008; Erickson *et al.*, 2011). Not only can oxidised CaMKII result in an increase in activity, but recent studies have also shown that O-linked glycosylation (another modification occurring in diabetes) of CaMKII can increase its activity (Erickson *et al.*, 2013).

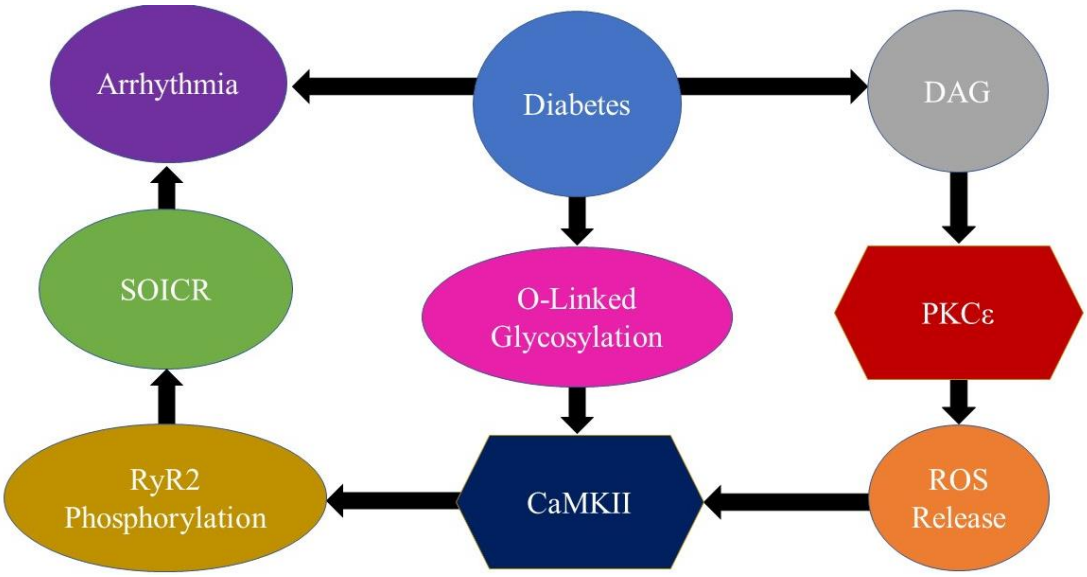

Figure 4.2 Proposed Model: PKCε Activation of CaMKII Links DM to Arrhythmia. DM has an increase accumulation of DAG which over activates PKCε. PKCε activates NOX2 increase ROS production and release increase CaMKII activation. Hyperglycemic environment in DM results in O-linked glycosylation of CaMKII increasing its activation. Hyper activation of CaMKII results in phosphorylation of RyR2 allowing for SOICR which leads to arrhythmia.

4.2.3 Oxidation of RyR2

Oxidation of the RyR2 has been shown to lead to a reduction of the release threshold resulting in SOICR, therefore, the increased occurrence of SOICR when there is overexpression of PKCε may be due to the activation of NOX2 causing ROS production and release, which then could result in the oxidation of RyR2 (Mi *et al.*, 2015; Waddell *et al.*, 2016).

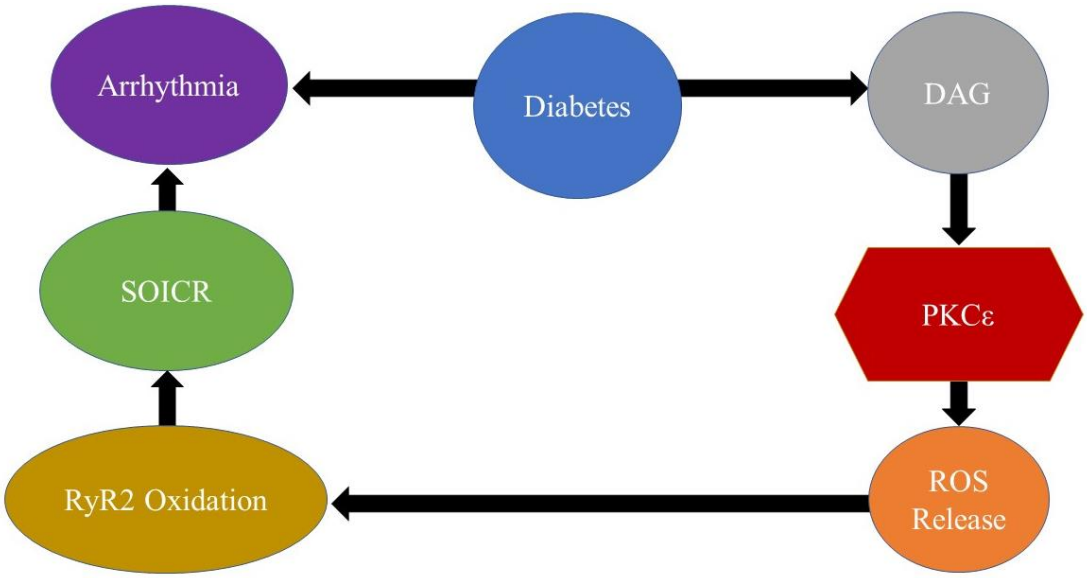

Figure 4.3 Proposed Model: PKCε Mediated Oxidation of RyR2 Links DM to arrhythmia. DM has an increase accumulation of DAG which over activates PKCε. PKCε activates NOX2 increase ROS production. The increase in ROS can lead to oxidation of RyR2 allowing for SOICR which leads to arrhythmia.

Overall, I propose that there are three possible models by which PKCε may result in a reduction of release threshold along with increased SOICR as seen in my study. To determine the most probable mode in which PKCε acts to increase SOICR, overexpression of PKCε with either; anti-oxidants to prevent oxidation of CaMKII or RyR2 by reducing ROS, CaMKII inhibitor (KN-93) to prevent CaMKII phosphorylation of RyR2 by preventing the dissociation of the autoinhibitory regulatory domain from the catalytic domain, or NOX2 inhibitor (Apocynin) to prevent ROS production by preventing the assembly of the NOX2 subunits (Birben *et al.*, 2012; Pellicena & Schulman, 2014; Qin *et al.*, 2017). If there is still a reduction in release threshold with increased SOICR when using an anti-oxidant, KN-93 and Phox-l2, then I would accept the proposed model in Figure 4.1. If, however, the use of KN-93 results abolishes the effect, PKCε would most likely be due to the activation of CaMKII, therefore, I would accept the proposed model in Figure 4.2. If the effect is still seen with KN-93 but abolished or reduced significantly with Apocynin, I would accept the proposed model in Figure 4.3. It is also possible that all three proposed models work together simultaneously.

4.3 Limitations

In my study I used HEK293 cells expressing RyR2 where the dynamics of Ca^{2+} release and entry were directly mediated by RyR2 and SERCA respectively, therefore, changes seen in SOICR could directly be linked to RyR2 mediated changes. However, in a cardiomyocyte, there are many other Ca^{2+} handling proteins that can be altered which could affect SOICR or the accumulation of Ca^{2+} within the cytosol. Currently, what is known about PKC role in the activity of other Ca^{2+} handling proteins is that PKCα in heart failure has been shown to phosphorylate protein phosphatase 1 (PP1), activating it, resulting in hypophosphorylation of PLB, thereby decreasing SERCA function (Braz *et al.*, 2004). The effect of PKC, regardless of isoform, on other Ca^{2+} handling proteins such as LTCC, NCX and Ca^{2+}-ATPase are not yet established, therefore, I must interpret results found in future studies on PKC in animal or human cardiac tissue with consideration of the multifaceted system.

Due to time constraints, I was unable to complete an ideal suite of experiments. To complete my study, it would be prudent to perform the following additional work:

1) Western blot analysis looking at total RyR2, PKCε and GAPDH using cell lysates from HEK293 cells transfected with PKCε to confirm transfection efficiency and that PKCε does not change RyR2 expression.
2) Luminal Ca^{2+} imaging to determine if Dic8 alone reduces the release threshold for SOICR, mentioned in Section 4.1.3.
3) Cytosolic and luminal Ca^{2+} imaging using Calphostin C to determine the effect of ATP-based kinase inhibitor independent inhibition of endogenous PKC on SOICR.

4.4 Future Steps

4.4.1 Cellular Studies

To determine if the effect of Dic8 was specific to one of the subclasses, the use of a broad spectrum nPKC or cPKC (Bisindolylmaleimide) inhibitor could be used along with Dic8 (Hers *et al.*, 1999). If the nPKC inhibitor or Bisindolylmaleimide attenuates the increase in SOICR seen by Dic8, then it is most likely the subclass being activated with Dic8 resulting in an increase in SOICR occurrence. The development of a broad nPKC inhibitor is required.

To confirm my hypothesis that RyR2 phosphorylation by PKC is what results in the decreased release threshold and thus the increased SOICR occurrence, western blotting looking at total phosphorylation of RyR2 using an antibody that binds specifically to phosphorylated residues normalised to total RyR2 would be required. I could then compare RyR2 phosphorylation levels between PKCα, PKCε, and mock transfected HEK293 cell lysates. As my results showed a decreased release threshold and termination threshold as well as an increase in SOICR occurrence with PKCε transfected HEK293 cells, I would expect an increase in total RyR2 phosphorylation compared to the mock transfected cells, where I would expect to see little/no change in total RyR2 phosphorylation due to PKCα. If results show an increase in RyR2 phosphorylation, the next step would then be to determine the site of phosphorylation. One way is to use bioinformatics (software/websites) to predict possibly PKC phosphorylation sites within RyR2 that matches the consensus sequence (Bauerova-Hlinkova *et al.*, 2010; Gao *et al.*, 2010). The presence/ absence of these sites can then be confirmed using mass spectrometry (Dephoure *et al.*, 2013). The sites can then be manipulated using site-directed mutagenesis to perform functional studies and specific antibodies can be developed that target these sites of interest to understand the level of phosphorylation (Carter, 1986; Goto & Inagaki, 2007).

In many proposed models of RyR2, there is a certain phosphorylation 'hot spot' where three residues have been proposed to be phosphorylated by PKA, CaMKII, and PKG (Valdivia, 2012). Due to the intensive research into RyR2 phosphorylation at these sites, HEK293 cell models expressing mutant forms of RyR2 have been developed where serine is replaced by alanine at the proposed phosphorylation target to prevent phosphorylation (Meng *et al.*, 2007). To determine if one of these three sites is a potential site of phosphorylation, the increase of SOICR occurrence due to PKCε transfection, would be diminished or abolished when using these HEK293 cell mutants with either one, two, or all three sites being altered from serine to alanine.

Along with PKCα and PKCε, PKCβ_2 and PKCδ have also been shown to be expressed in the heart and also have an increased activity or expression in DM (Borghini *et al.*, 1994). Using the same experimental design as this study examining the effect of PKCβ_2 and PKCδ could give further insight into which isoform results in the highest promotion of SOICR, in order to propose a potential therapeutic target in DM, as well as if RyR2 phosphorylation is also dependent on the subclass rather than the isoform (PKCβ_2 and PKCδ are cPKC and nPKC respectively). One thing that must be considered is that each isoform may be phosphorylating the RyR2 at different rates and at different sites all with different effects making the model yet more complicated.

4.4.2 Animal Studies

Following from cellular studies, the next step would be to determine the effect of PKC mediated SOICR in rat cardiomyocytes. Not only have DM rats been shown to have an increased risk of arrhythmia, they also show an increase in Ca^{2+} leak within the cardiomyocytes compared to non-DM (Smogorzewski *et al.*, 1998; Movahed *et al.*, 2005; Yaras *et al.*, 2005). For my experiment, rat hearts of DM and non-DM would be excised and cardiomyocytes would be

isolated using enzymatic digestion. These isolated cardiomyocytes would then be loaded with a cytosolic Ca^{2+} indicator dye, where cytosolic Ca^{2+} imaging would be performed to determine the occurrence of SOICR (Mu *et al.*, 2014). Therefore, my experiment would be to see the effect of SOICR in DM rat cardiomyocytes treated with a PKC inhibitor. I would expect that in the DM rat cardiomyocytes, PKC inhibition would attenuate the increased occurrence in SOICR, reducing the SOICR release similar to that of the non-DM rat. As my study showed that PKCε increases SOICR, I would test the effect of PKCε inhibitor peptide that inhibits the translocation of the active PKCε.

Functional effects of PKC inhibitors can also be used to see the generation of arrhythmia. DM rats experiencing arrhythmogenic events, seen on an electrocardiography would be treated with PKC inhibitors, where the occurrence of arrhythmic events would be compared between pre-treatment and post-treatment. Here I would expect to see a reduction in arrhythmogenic events in the post-treatment.

4.5 Summary

In summary, my results suggest that PKCε causes a reduction in the release threshold and termination threshold, thereby resulting in an increase in the occurrence SOICR. The way in which PKCε does this may either be through direct phosphorylation of RyR2, indirect phosphorylation of RyR2 through the oxidation-activation of CaMKII, or oxidation-activation of RyR2. PKCε is not only highly expressed in the heart, but it has increased activation in DM, therefore, it may be a novel link between DM and arrhythmia.

References

Adrover M, Vilanova B, Frau J, Munoz F & Donoso J. (2008). The pyridoxamine action on Amadori compounds: A reexamination of its scavenging capacity and chelating effect. *Bioorg Med Chem* **16,** 5557-5569.

Aebi M. (2013). N-linked protein glycosylation in the ER. *Biochim Biophys Acta* **1833,** 2430-2437.

Alonso-Moran E, Orueta JF, Fraile Esteban JI, Arteagoitia Axpe JM, Marques Gonzalez ML, Toro Polanco N, Ezkurra Loiola P, Gaztambide S & Nuno-Solinis R. (2014). The prevalence of diabetes-related complications and multimorbidity in the population with type 2 diabetes mellitus in the Basque Country. *BMC Public Health* **14,** 1059.

Aronsen JM, Swift F & Sejersted OM. (2013). Cardiac sodium transport and excitation-contraction coupling. *J Mol Cell Cardiol* **61,** 11-19.

Aschar-Sobbi R, Emmett TL, Kargacin GJ & Kargacin ME. (2012). Phospholamban phosphorylation increases the passive calcium leak from cardiac sarcoplasmic reticulum. *Pflugers Arch* **464,** 295-305.

Ayo SH, Radnik R, Garoni JA, Troyer DA & Kreisberg JI. (1991). High glucose increases diacylglycerol mass and activates protein kinase C in mesangial cell cultures. *Am J Physiol* **261,** F571-577.

Bauerova-Hlinkova V, Hostinova E, Gasperik J, Beck K, Borko L, Lai FA, Zahradnikova A & Sevcik J. (2010). Bioinformatic mapping and production of recombinant N-terminal domains of human cardiac ryanodine receptor 2. *Protein Expr Purif* **71,** 33-41.

Belke DD, Swanson EA & Dillmann WH. (2004). Decreased sarcoplasmic reticulum activity and contractility in diabetic db/db mouse heart. *Diabetes* **53,** 3201-3208.

Bers DM. (2002). Cardiac excitation-contraction coupling. *Nature* **415,** 198-205.

Bers DM. (2004). Macromolecular complexes regulating cardiac ryanodine receptor function. *J Mol Cell Cardiol* **37,** 417-429.

Birben E, Sahiner UM, Sackesen C, Erzurum S & Kalayci O. (2012). Oxidative stress and antioxidant defense. *World Allergy Organ J* **5,** 9-19.

Bodiga VL, Eda SR & Bodiga S. (2014). Advanced glycation end products: role in pathology of diabetic cardiomyopathy. *Heart Fail Rev* **19,** 49-63.

Borghini I, Ania-Lahuerta A, Regazzi R, Ferrari G, Gjinovci A, Wollheim CB & Pralong WF. (1994). Alpha, beta I, beta II, delta, and epsilon protein kinase C isoforms and compound activity in the sciatic nerve of normal and diabetic rats. *J Neurochem* **62,** 686-696.

Braz JC, Gregory K, Pathak A, Zhao W, Sahin B, Klevitsky R, Kimball TF, Lorenz JN, Nairn AC, Liggett SB, Bodi I, Wang S, Schwartz A, Lakatta EG, DePaoli-Roach AA, Robbins J, Hewett TE, Bibb JA, Westfall MV, Kranias EG & Molkentin JD. (2004). PKC-alpha

regulates cardiac contractility and propensity toward heart failure. *Nat Med* **10,** 248-254.

Carter P. (1986). Site-directed mutagenesis. *Biochem J* **237,** 1-7.

Dephoure N, Gould KL, Gygi SP & Kellogg DR. (2013). Mapping and analysis of phosphorylation sites: a quick guide for cell biologists. *Mol Biol Cell* **24,** 535-542.

Eisner D, Bode E, Venetucci L & Trafford A. (2013). Calcium flux balance in the heart. *J Mol Cell Cardiol* **58,** 110-117.

Erickson JR. (2014). Mechanisms of CaMKII Activation in the Heart. *Front Pharmacol* **5,** 59.

Erickson JR, He BJ, Grumbach IM & Anderson ME. (2011). CaMKII in the cardiovascular system: sensing redox states. *Physiol Rev* **91,** 889-915.

Erickson JR, Joiner ML, Guan X, Kutschke W, Yang J, Oddis CV, Bartlett RK, Lowe JS, O'Donnell SE, Aykin-Burns N, Zimmerman MC, Zimmerman K, Ham AJ, Weiss RM, Spitz DR, Shea MA, Colbran RJ, Mohler PJ & Anderson ME. (2008). A dynamic pathway for calcium-independent activation of CaMKII by methionine oxidation. *Cell* **133,** 462-474.

Erickson JR, Pereira L, Wang L, Han G, Ferguson A, Dao K, Copeland RJ, Despa F, Hart GW, Ripplinger CM & Bers DM. (2013). Diabetic hyperglycaemia activates CaMKII and arrhythmias by O-linked glycosylation. *Nature* **502,** 372-376.

Eshete F, Chung H, Gannon-Murakami L & Murakami K. (1998). Ca2+ modulation of cis-unsaturated fatty acid-induced mutant protein kinase C activity: indication of inhibitory Ca2+-binding site in protein kinase C-alpha. *Biochem J* **333 (Pt 1),** 215-221.

Fischer TH, Herting J, Mason FE, Hartmann N, Watanabe S, Nikolaev VO, Sprenger JU, Fan P, Yao L, Popov AF, Danner BC, Schondube F, Belardinelli L, Hasenfuss G, Maier LS & Sossalla S. (2015). Late INa increases diastolic SR-Ca2+-leak in atrial myocardium by activating PKA and CaMKII. *Cardiovasc Res* **107,** 184-196.

Gao J, Thelen JJ, Dunker AK & Xu D. (2010). Musite, a tool for global prediction of general and kinase-specific phosphorylation sites. *Mol Cell Proteomics* **9,** 2586-2600.

Geraldes P & King GL. (2010). Activation of protein kinase C isoforms and its impact on diabetic complications. *Circ Res* **106,** 1319-1331.

Goto H & Inagaki M. (2007). Production of a site- and phosphorylation state-specific antibody. *Nat Protoc* **2,** 2574-2581.

Grace AA & Roden DM. (2012). Systems biology and cardiac arrhythmias. *Lancet* **380,** 1498-1508.

Graham FL & van der Eb AJ. (1973). A new technique for the assay of infectivity of human adenovirus 5 DNA. *Virology* **52,** 456-467.

Grundy SM, Benjamin IJ, Burke GL, Chait A, Eckel RH, Howard BV, Mitch W, Smith SC, Jr. & Sowers JR. (1999). Diabetes and cardiovascular disease: a statement for healthcare professionals from the American Heart Association. *Circulation* **100,** 1134-1146.

Hers I, Tavare JM & Denton RM. (1999). The protein kinase C inhibitors bisindolylmaleimide I (GF 109203x) and IX (Ro 31-8220) are potent inhibitors of glycogen synthase kinase-3 activity. *FEBS Lett* **460,** 433-436.

Ho HT, Liu B, Snyder JS, Lou Q, Brundage EA, Velez-Cortes F, Wang H, Ziolo MT, Anderson ME, Sen CK, Wehrens XH, Fedorov VV, Biesiadecki BJ, Hund TJ & Gyorke S. (2014). Ryanodine receptor phosphorylation by oxidized CaMKII contributes to the cardiotoxic effects of cardiac glycosides. *Cardiovasc Res* **101,** 165-174.

Hongpaisan J, Sun MK & Alkon DL. (2011). PKC epsilon activation prevents synaptic loss, Abeta elevation, and cognitive deficits in Alzheimer's disease transgenic mice. *J Neurosci* **31,** 630-643.

Houser SR. (2000). When does spontaneous sarcoplasmic reticulum CA(2+) release cause a triggered arrythmia? Cellular versus tissue requirements. *Circ Res* **87,** 725-727.

Huke S & Bers DM. (2008). Ryanodine receptor phosphorylation at Serine 2030, 2808 and 2814 in rat cardiomyocytes. *Biochem Biophys Res Commun* **376,** 80-85.

Jones PP, Jiang D, Bolstad J, Hunt DJ, Zhang L, Demaurex N & Chen SR. (2008). Endoplasmic reticulum Ca2+ measurements reveal that the cardiac ryanodine receptor mutations linked to cardiac arrhythmia and sudden death alter the threshold for store-overload-induced Ca2+ release. *Biochem J* **412,** 171-178.

Kamato D, Mitra P, Davis F, Osman N, Chaplin R, Cabot PJ, Afroz R, Thomas W, Zheng W, Kaur H, Brimble M & Little PJ. (2017). Gaq proteins: molecular pharmacology and therapeutic potential. *Cell Mol Life Sci* **74,** 1379-1390.

Kania E, Roest G, Vervliet T, Parys JB & Bultynck G. (2017). IP3 Receptor-Mediated Calcium Signaling and Its Role in Autophagy in Cancer. *Front Oncol* **7,** 140.

Kirwan AF, Bibby AC, Mvilongo T, Riedel H, Burke T, Millis SZ & Parissenti AM. (2003). Inhibition of protein kinase C catalytic activity by additional regions within the human protein kinase Calpha-regulatory domain lying outside of the pseudosubstrate sequence. *Biochem J* **373,** 571-581.

Kobayashi E, Nakano H, Morimoto M & Tamaoki T. (1989). Calphostin C (UCN-1028C), a novel microbial compound, is a highly potent and specific inhibitor of protein kinase C. *Biochem Biophys Res Commun* **159,** 548-553.

Kohlhaas M, Zhang T, Seidler T, Zibrova D, Dybkova N, Steen A, Wagner S, Chen L, Brown JH, Bers DM & Maier LS. (2006). Increased sarcoplasmic reticulum calcium leak but unaltered contractility by acute CaMKII overexpression in isolated rabbit cardiac myocytes. *Circ Res* **98,** 235-244.

Kong H, Jones PP, Koop A, Zhang L, Duff HJ & Chen SR. (2008). Caffeine induces Ca2+ release by reducing the threshold for luminal Ca2+ activation of the ryanodine receptor. *Biochem J* **414,** 441-452.

Liao MH, Xiang YC, Huang JY, Tao RR, Tian Y, Ye WF, Zhang GS, Lu YM, Ahmed MM, Liu ZR, Fukunaga K & Han F. (2013). The disturbance of hippocampal CaMKII/PKA/PKC phosphorylation in early experimental diabetes mellitus. *CNS Neurosci Ther* **19,** 329-336.

Liu Y, Kimlicka L, Hiess F, Tian X, Wang R, Zhang L, Jones PP, Van Petegem F & Chen SR. (2013). The CPVT-associated RyR2 mutation G230C enhances store overload-induced Ca2+ release and destabilizes the N-terminal domains. *Biochem J* **454,** 123-131.

Liu Y, Wei J, Wong King Yuen SM, Sun B, Tang Y, Wang R, Van Petegem F & Chen SRW. (2017). CPVT-associated cardiac ryanodine receptor mutation G357S with reduced penetrance impairs Ca2+ release termination and diminishes protein expression. *PLoS One* **12,** e0184177.

Maurya AK & Vinayak M. (2015). Modulation of PKC signaling and induction of apoptosis through suppression of reactive oxygen species and tumor necrosis factor receptor 1 (TNFR1): key role of quercetin in cancer prevention. *Tumour Biol* **36,** 8913-8924.

McCauley MD & Wehrens XH. (2011). Ryanodine receptor phosphorylation, calcium/calmodulin-dependent protein kinase II, and life-threatening ventricular arrhythmias. *Trends Cardiovasc Med* **21,** 48-51.

Meng X, Xiao B, Cai S, Huang X, Li F, Bolstad J, Trujillo R, Airey J, Chen SR, Wagenknecht T & Liu Z. (2007). Three-dimensional localization of serine 2808, a phosphorylation site in cardiac ryanodine receptor. *J Biol Chem* **282,** 25929-25939.

Mi T, Xiao Z, Guo W, Tang Y, Hiess F, Xiao J, Wang Y, Zhang JZ, Zhang L, Wang R, Jones PP & Chen SR. (2015). Role of Cys(3)(6)(0)(2) in the function and regulation of the cardiac ryanodine receptor. *Biochem J* **467,** 177-190.

Mochly-Rosen D, Das K & Grimes KV. (2012). Protein kinase C, an elusive therapeutic target? *Nat Rev Drug Discov* **11,** 937-957.

Movahed MR, Hashemzadeh M & Jamal MM. (2005). Diabetes mellitus is a strong, independent risk for atrial fibrillation and flutter in addition to other cardiovascular disease. *Int J Cardiol* **105,** 315-318.

Mu YH, Zhao WC, Duan P, Chen Y, Zhao WD, Wang Q, Tu HY & Zhang Q. (2014). RyR2 modulates a Ca2+-activated K+ current in mouse cardiac myocytes. *PLoS One* **9,** e94905.

Murillo-Carretero M, Geribaldi-Doldán N, Flores-Giubi E, García-Bernal F, Navarro-Quiroz E, Carrasco M, Macías-Sánchez A, Herrero-Foncubierta P, Delgado-Ariza A, Verástegui C, Domínguez-Riscart J, Daoubi M, Hernández-Galán R & Castro C (2017). ELAC (3,12-di-O-acetyl-8-O-tigloilingol), a plant-derived lathyrane diterpene, induces subventricular zone neural progenitor cell proliferation through PKCβ activation. *British Journal of Pharmacology* **174**, 2373-2392.

NCD Risk Factor Collaboration. (2016). Worldwide trends in diabetes since 1980: a pooled analysis of 751 population-based studies with 4.4 million participants. *Lancet* **387,** 1513-1530.

New DC & Wong YH. (2007). Molecular mechanisms mediating the G protein-coupled receptor regulation of cell cycle progression. *J Mol Signal* **2,** 2.

Newton AC. (2003). Regulation of the ABC kinases by phosphorylation: protein kinase C as a paradigm. *Biochem J* **370,** 361-371.

Newton AC, Antal CE & Steinberg SF. (2016). Protein kinase C mechanisms that contribute to cardiac remodelling. *Clin Sci (Lond)* **130,** 1499-1510.

Overend CL, Eisner DA & O'Neill SC. (1997). The effect of tetracaine on spontaneous Ca2+ release and sarcoplasmic reticulum calcium content in rat ventricular myocytes. *J Physiol* **502 (Pt 3),** 471-479.

Palade P, Mitchell RD & Fleischer S. (1983). Spontaneous calcium release from sarcoplasmic reticulum. General description and effects of calcium. *J Biol Chem* **258,** 8098-8107.

Pellicena P & Schulman H. (2014). CaMKII inhibitors: from research tools to therapeutic agents. *Front Pharmacol* **5,** 21.

Pieters M, van Zyl DG, Rheeder P, Jerling JC, Loots du T, van der Westhuizen FH, Gottsche LT & Weisel JW. (2007). Glycation of fibrinogen in uncontrolled diabetic patients and the effects of glycaemic control on fibrinogen glycation. *Thromb Res* **120,** 439-446.

Ping P, Zhang J, Qiu Y, Tang XL, Manchikalapudi S, Cao X & Bolli R. (1997). Ischemic preconditioning induces selective translocation of protein kinase C isoforms epsilon and eta in the heart of conscious rabbits without subcellular redistribution of total protein kinase C activity. *Circ Res* **81,** 404-414.

Puttaiah S, Zhang Y, Pilch HA, Pfahler C, Oya-Ito T, Sayre LM & Nagaraj RH. (2006). Detection of dideoxyosone intermediates of glycation using a monoclonal antibody: characterization of major epitope structures. *Arch Biochem Biophys* **446,** 186-196.

Qin YY, Li M, Feng X, Wang J, Cao L, Shen XK, Chen J, Sun M, Sheng R, Han F & Qin ZH. (2017). Combined NADPH and the NOX inhibitor apocynin provides greater anti-inflammatory and neuroprotective effects in a mouse model of stroke. *Free Radic Biol Med* **104,** 333-345.

Saffitz JE. (2005). Dependence of electrical coupling on mechanical coupling in cardiac myocytes: insights gained from cardiomyopathies caused by defects in cell-cell connections. *Ann N Y Acad Sci* **1047,** 336-344.

Sakwe AM, Larsson M & Rask L. (2004). Involvement of protein kinase C-alpha and -epsilon in extracellular Ca(2+) signalling mediated by the calcium sensing receptor. *Exp Cell Res* **297,** 560-573.

Sakwe AM, Rask L & Gylfe E. (2005). Protein kinase C modulates agonist-sensitive release of Ca2+ from internal stores in HEK293 cells overexpressing the calcium sensing receptor. *J Biol Chem* **280,** 4436-4441.

Sandow A. (1952). Excitation-contraction coupling in muscular response. *Yale J Biol Med* **25,** 176-201.

Shan J, Xie W, Betzenhauser M, Reiken S, Chen BX, Wronska A & Marks AR. (2012). Calcium leak through ryanodine receptors leads to atrial fibrillation in 3 mouse models of catecholaminergic polymorphic ventricular tachycardia. *Circ Res* **111,** 708-717.

Simonis G, Briem SK, Schoen SP, Bock M, Marquetant R & Strasser RH. (2007). Protein kinase C in the human heart: differential regulation of the isoforms in aortic stenosis or dilated cardiomyopathy. *Mol Cell Biochem* **305,** 103-111.

Siscovick DS, Sotoodehnia N, Rea TD, Raghunathan TE, Jouven X & Lemaitre RN. (2010). Type 2 diabetes mellitus and the risk of sudden cardiac arrest in the community. *Rev Endocr Metab Disord* **11,** 53-59.

Smogorzewski M, Galfayan V & Massry SG. (1998). High glucose concentration causes a rise in [Ca2+]i of cardiac myocytes. *Kidney Int* **53,** 1237-1243.

Stahelin RV, Digman MA, Medkova M, Ananthanarayanan B, Melowic HR, Rafter JD & Cho W. (2005). Diacylglycerol-induced membrane targeting and activation of protein kinase Cepsilon: mechanistic differences between protein kinases Cdelta and Cepsilon. *J Biol Chem* **280,** 19784-19793.

Steinberg SF. (2012). Cardiac actions of protein kinase C isoforms. *Physiology (Bethesda)* **27,** 130-139.

Stitt AW, Moore JE, Sharkey JA, Murphy G, Simpson DA, Bucala R, Vlassara H & Archer DB. (1998). Advanced glycation end products in vitreous: Structural and functional implications for diabetic vitreopathy. *Invest Ophthalmol Vis Sci* **39,** 2517-2523.

Takasago T, Imagawa T, Furukawa K, Ogurusu T & Shigekawa M. (1991). Regulation of the cardiac ryanodine receptor by protein kinase-dependent phosphorylation. *J Biochem* **109,** 163-170.

Tang Y, Tian X, Wang R, Fill M & Chen SR. (2012). Abnormal termination of Ca2+ release is a common defect of RyR2 mutations associated with cardiomyopathies. *Circ Res* **110,** 968-977.

Valdivia HH. (2012). Ryanodine receptor phosphorylation and heart failure: phasing out S2808 and "criminalizing" S2814. *Circ Res* **110,** 1398-1402.

Van Petegem F. (2015). Ryanodine receptors: allosteric ion channel giants. *J Mol Biol* **427,** 31-53.

Venetucci LA, Trafford AW, O'Neill SC & Eisner DA. (2007). Na/Ca exchange: regulator of intracellular calcium and source of arrhythmias in the heart. *Ann N Y Acad Sci* **1099,** 315-325.

Waddell HMM, Zhang JZ, Hoeksema KJ, McLachlan JJ, McLay JC & Jones PP. (2016). Oxidation of RyR2 Has a Biphasic Effect on the Threshold for Store Overload-Induced Calcium Release. *Biophys J* **110,** 2386-2396.

Wagner S, Maier LS & Bers DM. (2015). Role of sodium and calcium dysregulation in tachyarrhythmias in sudden cardiac death. *Circ Res* **116,** 1956-1970.

Wehrens XH, Lehnart SE, Reiken S, Vest JA, Wronska A & Marks AR. (2006). Ryanodine receptor/calcium release channel PKA phosphorylation: a critical mediator of heart failure progression. *Proc Natl Acad Sci U S A* **103,** 511-518.

Wiley J (2011). The Conduction System of the Heart. *Higheredbcswileycom*. Available at: http://higheredbcs.wiley.com/legacy/college/tortora/0470565101/hearthis_ill/pap13e_ch20_illustr_audio_mp3_am/simulations/hear/heart_conduction.html [Accessed May 31, 2017]

Xia P, Inoguchi T, Kern TS, Engerman RL, Oates PJ & King GL. (1994). Characterization of the mechanism for the chronic activation of diacylglycerol-protein kinase C pathway in diabetes and hypergalactosemia. *Diabetes* **43,** 1122-1129.

Xiao B, Tian X, Xie W, Jones PP, Cai S, Wang X, Jiang D, Kong H, Zhang L, Chen K, Walsh MP, Cheng H & Chen SR. (2007). Functional consequence of protein kinase A-dependent phosphorylation of the cardiac ryanodine receptor: sensitization of store overload-induced Ca2+ release. *J Biol Chem* **282,** 30256-30264.

Xiao H & Liu M. (2013). Atypical protein kinase C in cell motility. *Cell Mol Life Sci* **70,** 3057-3066.

Yaras N, Ugur M, Ozdemir S, Gurdal H, Purali N, Lacampagne A, Vassort G & Turan B. (2005). Effects of diabetes on ryanodine receptor Ca release channel (RyR2) and Ca2+ homeostasis in rat heart. *Diabetes* **54,** 3082-3088.

Zhang D & Aravind L. (2010). Identification of novel families and classification of the C2 domain superfamily elucidate the origin and evolution of membrane targeting activities in eukaryotes. *Gene* **469,** 18-30.

Zhang JZ, Waddell HM & Jones PP. (2015). Regulation of RYR2 by sarcoplasmic reticulum Ca(2+). *Clin Exp Pharmacol Physiol* **42,** 720-726.

Zhang P, Smith-Nguyen EV, Keshwani MM, Deal MS, Kornev AP & Taylor SS. (2012). Structure and allostery of the PKA RIIbeta tetrameric holoenzyme. *Science* **335,** 712-716.

Zimmet P, Alberti KG & Shaw J. (2001). Global and societal implications of the diabetes epidemic. *Nature* **414,** 782-787.